

Chapter 10

The Cytochrome *b₆f* Complex: Biophysical Aspects of Its Functioning in Chloroplasts



Alexander N. Tikhonov

Abstract This chapter presents an overview of structural properties of the cytochrome (Cyt) *b₆f* complex and its functioning in chloroplasts. The Cyt *b₆f* complex stands at the crossroad of photosynthetic electron transport pathways, providing connectivity between Photosystem (PSI) and Photosystem II (PSII) and pumping protons across the membrane into the thylakoid lumen. After a brief review of the chloroplast electron transport chain, the consideration is focused on the structural organization of the Cyt *b₆f* complex and its interaction with plastoquinol (PQH₂, reduced form of plastoquinone), a mediator of electron transfer from PSII to the Cyt *b₆f* complex. The processes of PQH₂ oxidation by the Cyt *b₆f* complex have been considered within the framework of the Mitchell's Q-cycle. The overall rate of the intersystem electron transport is determined by PQH₂ turnover at the quinone-binding site Q_o of the Cyt *b₆f* complex. The rate of PQH₂ oxidation is controlled by the intrathylakoid pH_{in}, which value determines the protonation/deprotonation events in the Q_o-center. Two other regulatory mechanisms associated with the Cyt *b₆f* complex are briefly overviewed: (i) redistribution of electron fluxes between alternative (linear and cyclic) pathways, and (ii) "state transitions" related to redistribution of solar energy between PSI and PSII.

Keywords Photosynthesis · Chloroplasts · Electron transport control · Cytochrome *b₆f* complex · Plastoquinone

A. N. Tikhonov (✉)

Faculty of Physics, Moscow State University, Moscow, Russia

e-mail: an_tikhonov@mail.ru

© Springer Nature Singapore Pte Ltd. 2018

J. R. Harris, E. J. Boekema (eds.), *Membrane Protein Complexes: Structure and Function*, Subcellular Biochemistry 87,

https://doi.org/10.1007/978-981-10-7757-9_10

Abbreviations

CBC	Calvin-Benson cycle
CEF1	cyclic electron flow around photosystem I
ETC	electron transport chain
Fd	ferredoxin
FNR	ferredoxin-NADP-oxidoreductase
ISP	iron-sulfur protein
LEF	linear electron flow
LHCI	light-harvesting complex I
LHCII	light-harvesting complex II
NDH	NDH(P)H dehydrogenase complex
NPQ	non-photochemical quenching
P ₆₈₀	special chlorophyll pair in PSII
P ₇₀₀	special chlorophyll pair in PSI
Pc	plastocyanin
PCET	proton-coupled electron transfer
PQ and PQH ₂	plastoquinone and plastoquinol, respectively
PSA	photosynthetic apparatus
PSI and PSII	photosystem I and photosystem II respectively
Q, SQ and QH ₂	general notations for three accessible redox states of quinone species – quinone (Q), semiquinone (SQ) and quinol (QH ₂)
TMQH ₂	trimethylbenzoquinol
UQ and UQH ₂	ubiquinone and ubiquinol, respectively
WOC	water-oxidizing complex

10.1 Introduction

Photosynthesis is one of the most important processes in nature. Photosynthetic organisms of oxygenic type (cyanobacteria, algae, higher plants), using the solar energy, assimilate carbon dioxide and produce molecular oxygen. The energy of light quanta absorbed by the pigment-protein complexes of photosystem I (PSI) and photosystem II (PSII) is converted into the energy of separated charges in photoreaction centers (Blankenship 2002; Cardona et al. 2012; Müh et al. 2012; Ruban 2012; Mamedov et al. 2015). The light-driven actuation of photoreaction centers initiates electron transfer along the photosynthetic electron transport chain (ETC). Two electrons extracted from the water molecule split by the water-oxidizing complex (WOC) of PSII, are passed to the terminal electron acceptor of PSI, NADP⁺. PSI complex delivers electrons to NADP⁺ through ferredoxin (Fd) and ferredoxin-NADP-oxidoreductase (FNR): PSI → Fd → FNR → NADP⁺. The cytochrome (Cyt) *b₆f* complex is another multisubunit complex, which plays a crucial role in photosynthetic electron transport, because it stands at the crossroad of electron transport

pathways between PSII and PSI. These photosystems are interconnected via the membrane-bound Cyt *b₆f* complex and mobile electron carriers, plastoquinone (PQ), plastocyanin (Pc): $\text{H}_2\text{O} \rightarrow \text{PSII} \rightarrow \text{PQ} \rightarrow b_6f \rightarrow \text{Pc} \rightarrow \text{PSI}$. Electron transfer from H_2O to NADP^+ is accompanied by alkalization of stroma (the volume between the chloroplast envelope and thylakoids) and acidification of the *intra*-thylakoid lumen (the internal volume of thylakoids). The light-induced uptake of protons from the bulk of stroma and the proton release in the lumen lead to generation of the *trans*-thylakoid difference in electrochemical potentials of hydrogen ions, $\Delta\bar{m}_{\text{H}^+}$ (often termed as the proton-motive force), which serves as the driving force for operation of the ATP synthase complex $\text{CF}_0 - \text{CF}_1(\text{ADP} + \text{P}_i \rightarrow \text{ATP} + \text{H}_2\text{O})$ (Mitchell 1966; Blankenship 2002; Junge and Nelson 2015). The macroergic products of the light-induced stages of photosynthesis, ATP and NADPH, are used mainly in biosynthetic reactions of the Calvin-Benson cycle (CBC) (Edwards and Walker 1983; Blankenship 2002).

In this Chapter, the structural and functional properties of the Cyt *b₆f* complex are considered in the context of its interaction with PQH_2 (the double-reduced form of PQ) and feedback regulation of electron transport in chloroplasts. The reaction of PQH_2 oxidation by the Cyt *b₆f* complex represents the “bottle-neck” link in the ETC between PSII and PSI, which virtually determines the overall rate of the intersystem electron transport in chloroplasts. The redox state of the PQ pool plays the pivoting role in regulation of photosynthetic processes, because it serves the role of a peculiar “sensor” (for review, see Pesaresi et al. 2010) that triggers the short-term and long-term mechanisms of photosynthetic apparatus (PSA) response to varying environmental conditions (Kramer et al. 2004; Cruz et al. 2007; Eberhard et al. 2008; Demmig-Adams et al. 2012; Horton 2012; Rochaix 2014; Puthiyaveetil et al. 2016). The flexibility of PSA functioning in chloroplasts is achieved by cooperation of several feedback mechanisms of electron transport control. These regulatory mechanisms include different events: (i) pH-dependent control of PQH_2 oxidation by the Cyt *b₆f* complex, (ii) optimization of the light quanta partitioning between PSI and PSII (“state transitions”) triggered by the Cyt *b₆f* complex, and (iii) redistribution of electron fluxes through alternative pathways of electron transport. All these mechanisms are associated with the functioning of the Cyt *b₆f* complex.

10.2 Photosynthetic Electron Transport Chain

The multisubunit electron-transport complexes are embedded into lamellar membranes of thylakoids, closed vesicles situated under the chloroplast envelope. Figure 10.1 depicts a scheme of basic electron transport pathways in chloroplasts. The peculiarities of functioning photoreaction centers of PSI, PSII, and the Cyt *b₆f* complex are briefly considered below.

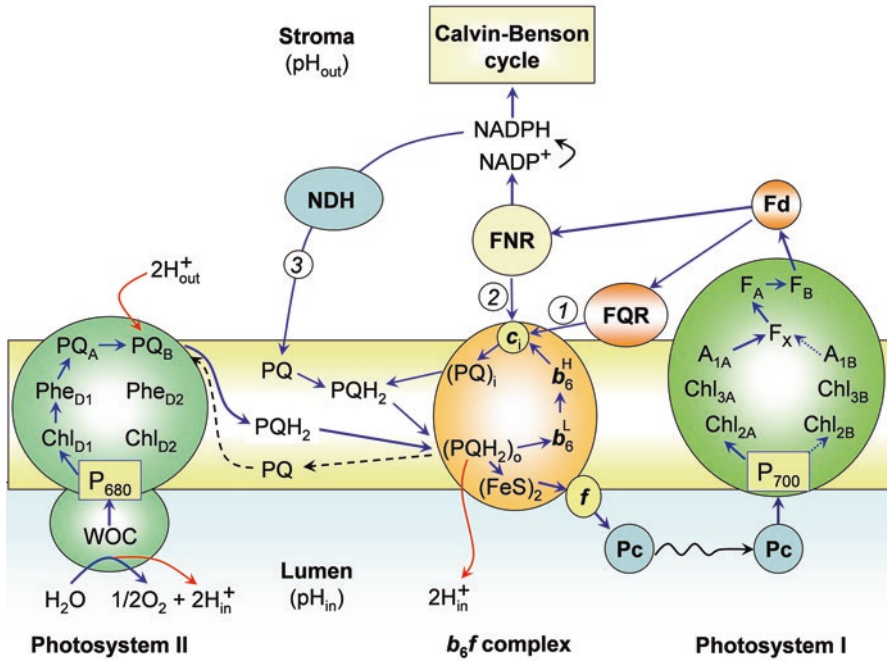


Fig. 10.1 A scheme of electron transport pathways in chloroplasts and the arrangement of protein complexes (Photosystem I, Photosystem II, Cyt b_6f , FNR, and NDH) in the thylakoid membrane. Two electrons extracted from the water molecule in Photosystem II are transferred to plastoquinone (PQ), reducing PQ to plastoquinol (PQH₂). Electrons from PQH₂ are transferred via the Cyt b_6f complex to reduce plastocyanin (Pc). Photosystem I oxidizes Pc on the luminal side of the thylakoid membrane and reduces ferredoxin (Fd) on the stromal side of the membrane. Reduced ferredoxin donates electrons to FNR, which provides the two-electron reduction of NADP⁺ to NADPH. Reduced and protonated NADPH molecules are consumed in the Calvin-Benson cycle. Electron transport processes are accompanied by accumulation of hydrogen ions in the thylakoid lumen (Modified from Figure 1 in Tikhonov 2014)

10.2.1 Photosystems I and II

Photosystem I The multisubunit pigment-protein PSI complex catalyzes electron transfer from Pc (or Cyt c_6 in cyanobacteria) on the luminal side of thylakoids to Fd (or flavodoxin) located in stroma (Brettel 1997; Jordan et al. 2001; Fromme et al. 2001; Nelson and Yocum 2006; Shelaev et al. 2010; Mamedov et al. 2015). Reduced ferredoxin (Fd⁻) passes an electron to FNR, which provides the two-electron reduction of NADP⁺ to NADPH. The core domain of the PSI complex contains a special pair of chlorophyll (Chl) a molecules (Chl_{1A} and Chl_{1B}) located at the interface of subunits PsaA and PsaB, which form the primary electron donor termed P₇₀₀. The light-induced excitation of P₇₀₀ induces charge separation in PSI: excited center P₇₀₀^{*} donates an electron to the primary electron acceptor (Chl_{2A} or Chl_{2B}). On the acceptor side of PSI, electron carriers are arranged as two quasi-symmetrical cofactor branches, which consist of two Chl a molecules (Chl_{2A} and Chl_{3A} in A-branch;

Chl_{2B} and Chl_{3B} in B-branch) and one phylloquinone molecule (A_{1A} or A_{1B}, respectively). The two branches converge at the acceptor F_X (one of three [FeS]₄ clusters of PSI, F_X, F_A, and F_B). There are experimental evidences in favor of preferential role of A-branch in electron transfer on the acceptor side of PSI (for references, see Mamedov et al. 2015). From reduced F_X the electron is transferred to Fd via the redox centers F_A and F_B (F_X → F_A → F_B → Fd). Reduced Fd molecules deliver electrons to NADP⁺ via FNR (Fig. 10.1).

Oxidized center P₇₀₀⁺ accepts an electron from reduced Pc (Pc⁻), which, in turn, accepts an electron from the Cyt *b₆f* complex. Pc serves the role of the electron transfer shuttle, which, moving within the lumen, connects electronically the Cyt *b₆f* complex and PSI. Lateral diffusion of Pc⁻ inside the lumen, and further donation of an electron from Pc⁻ to P₇₀₀⁺, do not limit electron transport between PSII and PSI. Oxidation of Pc⁻ by P₇₀₀⁺ occurs more rapidly (*t*_{1/2} < 200 μs, at ambient temperatures) than electron transfer from PSII to Pc via the PQ pool and Cyt *b₆f* complex (*t*_{1/2} ≥ 4 – 20 ms) (Stiehl and Witt 1969; Witt 1979; Haehnel 1984).

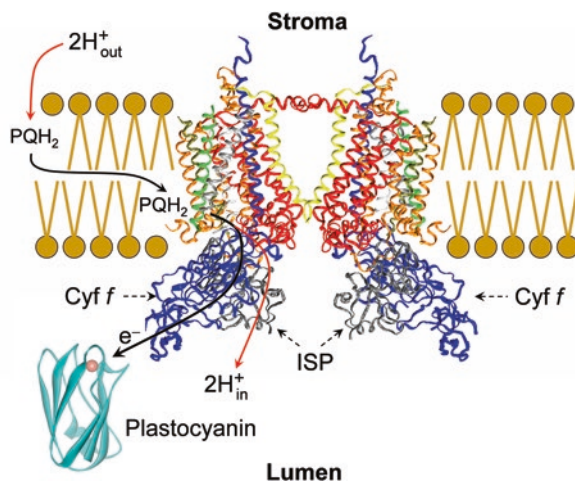
Photosystem II PSII contains the primary electron donor P₆₈₀ and the water-oxidizing complex (WOC). Two electrons extracted from H₂O in WOC (H₂O → 1/2O₂ + 2H⁺ + 2e⁻) are used to reduce PQ to PQH₂. Transfer of electrons from H₂O to PQ molecules proceeds as the result of consecutive one-electron reactions induced by light quanta absorbed by the light-harvesting antenna of PSII. A special pair of Chl *a* molecules embedded into the core of the PSII complex form the primary electron donor in PSII termed P₆₈₀ (for review, see Cardona et al. 2012, Müh et al. 2012). There are two branches of electron cofactors on the acceptor side of PSII, A-branch and B-branch. Excited redox center P₆₈₀^{*} donates an electron to the primary electron acceptor of A-branch, Chl *a* molecule termed Chl_{D1}, which, in its turn, passes the electron to the secondary acceptor pheophytin (Phe): P₆₈₀^{*} → Chl_{D1} → Phe_{D1}. Reduced Phe donates the electron to the primary plastoquinone PQ_A tightly bound to PSII (Phe⁻PQ_APQ_B → Phe PQ_A⁻PQ_B). PQ_A⁻ reduces the secondary plastoquinone PQ_B bound to PSII (PQ_A⁻PQ_B → PQ_APQ_B⁻). The second electron donated by P₆₈₀^{*} to PQ_A provides the double-electron reduction of PQ_B (PQ_A⁻PQ_B⁻ → PQ_APQ_B⁼), which is followed by protonation of PQ_B⁼ due to the uptake of two protons from stroma (PQ_B⁼ + 2H_{out}⁺ → PQ_BH₂). Reduced secondary plastoquinone, PQ_BH₂, dissociates from PSII in exchange for a new oxidized PQ molecule. Diffusing in the membrane, the hydrophobic PQH₂ molecule reaches the Cyt *b₆f* complex. After binding of PQH₂ to the Q_o-center of this complex, the PQH₂ molecule oxidizes, donating two electrons to appropriate electron acceptors of the Cyt *b₆f* complex and releasing two protons, which finally migrate into the bulk phase of the thylakoid lumen. On the donor side of PSII, decomposition of water molecules in the WOC is accompanied by the release of protons into the lumen. The overall balance of electron and proton transport processes in PSII is the following: (i) two electrons extracted from one H₂O molecule are used to reduce PQ to PQH₂, and (ii) two protons are taken up from stroma and two protons appear in the lumen per one PQH₂ molecule formed (H₂O + PQ + 2H_{out}⁺ → 1/2O₂ + PQH₂ + 2H_{in}⁺).

10.2.2 The Role of Cytochrome b_6f Complex in the Pathway Between Photosystems I and II

The Cyt b_6f complex (plastoquinol:plastocyanin oxidoreductase) is organized as the hetero-oligomeric protein complex, which mediates electron transfer between PSII and PSI by oxidizing PQH₂ and reducing Pc. Three-dimensional structures of this complex were initially obtained at a resolution of 3.0–3.1 Å from the thermophilic filamentous cyanobacterium *Mastigocladus laminosus* (PDB entry 1VF5; Kurisu et al. 2003), and the green alga *Chlamydomonas reinhardtii* (PDB entry 1Q90; Stroebel et al. 2003), in the presence of the quinone analogue inhibitor, tri-decylstigmatellin (TDS). The crystal structures of the Cyt b_6f complexes from *M. laminosus* and *C. reinhardtii* are similar. The Cyt b_6f complex is organized as the functional dimer of multisubunit monomers (Fig. 10.2). Dimeric organization of the Cyt b_6f complex is similar, in general, to that of the Cyt bc_1 complex of the Cyt bc family (Xia et al. 1997, 2013; Iwata et al. 1998; Berry et al. 2000; Crofts 2004a; Cramer et al. 2006, 2011). Each multisubunit monomer of the functional dimer of the Cyt b_6f complex consists of eight polypeptide subunits with 13 *trans*-membrane helices, including four “large” (16–31 kDa) polypeptide subunits (petA, B, C, and D): the iron-sulfur protein (ISP) Rieske, the Cyt b_6 and Cyt f proteins, and subunit IV (Fig. 10.3). “Small” (3.3–4.1 kDa) hydrophobic subunits (petG, L, M, and N), each of them containing one *trans*-membrane helix, are arranged at the outside periphery of the monomer ensemble of petA, B, C, and D subunits.

The catalytic functions of the Cyt b_6f complex are provided by four redox centers bound to the “large” subunits: the Rieske iron-sulfur cluster [Fe₂S₂], two hemes of the Cyt b_6 (the low-potential heme b_6^L and the high-potential heme b_6^H), and heme f of the Cyt f . These cofactors are involved in the electron transfer reactions within the Cyt b_6f complex. Furthermore, there are three unusual prosthetic groups: (1) Chl a , (2) β -carotene, and (3) a unique heme c_1 (Stroebel et al. 2003), which is often

Fig. 10.2 The side view of the dimeric Cyt b_6f complex from *Chlamydomonas reinhardtii* (PDB entry 1Q90, Stroebel et al. 2003). Figure was produced using Accelrys DV visualizer software package (<http://www.accelrys.com>) (Modified from Figure 2 in Tikhonov 2014)



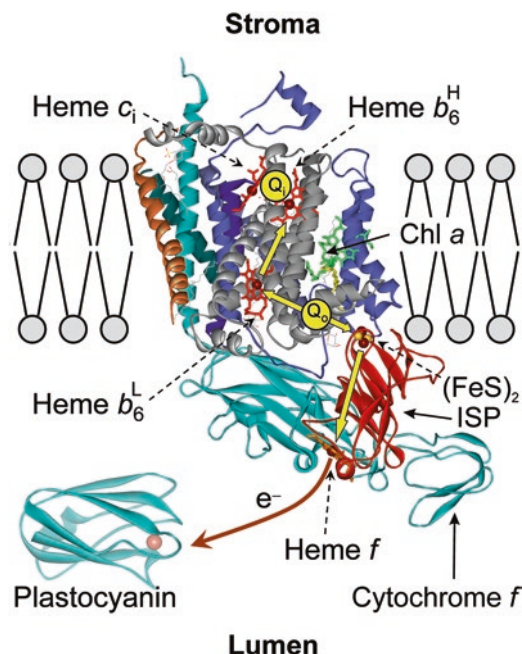


Fig. 10.3 Overview of structure and function of the Cyt b_6f complex from *Chlamydomonas reinhardtii* (PDB entry 1Q90, Stroebel et al. 2003). The view is perpendicular to the membrane plane. Colour code of main polypeptides: cyan, Cyt f ; grey, Cyt b_6 ; purple, the iron-sulfur protein; blue, subunit IV. Cofactors: red, hemes b_6^L , b_6^H , and c_1 , as indicated; orange, heme f ; Fe atoms are shown as dark red spheres; green, Chl a . Plastoquinone binding site Q_o is positioned between heme b_6^L and the $[\text{Fe}_2\text{S}_2]$ cluster of the iron-sulfur protein. Plastoquinone binding site Q_i is placed between hemes b_6^H and c_1 (Modified from Figure 3 in Tikhonov 2014. Figure was produced using Accelrys DV visualizer software package (<http://www.accelrys.com>))

termed as heme c_n because of its location on the “negative” side of the membrane (Kurisu et al. 2003). Heme $c_i(c_n)$ is bound covalently to the Cyt b_6f complex in close proximity to the high-potential heme b_6^H . The Cyt b_6 and Cyt f subunits are functionally analogous to the Cyt b_6 and Cyt c_1 proteins in the mitochondrial and bacterial Cyt bc_1 complexes (Xia et al. 1997, 2013; Iwata et al. 1998; Berry et al. 2000; Crofts 2004a). The Cyt b_6f complex contains the binding centers for PQH_2 and PQ molecules. Crystallization of the Cyt b_6f complexes with quinone analogue inhibitors, TDS and NQNO (*2n*-nonyl-4-hydroxy-quinoline-*N*-oxide) revealed two sites for quinone binding: the Q_o -center (quinol oxidase) and the Q_i -center (quinone reductase) (Yamashita et al. 2007). The quinone exchange cavity of the site Q_o is positioned near the $[\text{Fe}_2\text{S}_2]$ cluster of the ISP. Site Q_i is located on the stromal side of the complex, at the interface between heme c_i and the large inter-protein quinone exchange cavity.

Oxidation of PQH_2 occurs at the catalytic center Q_o , which is situated in the cavity at the interface between the Cyt b_6 subunit and the ISP. This center is oriented

towards the luminal side of the thylakoid membrane. The oxidation of PQH₂ in the Q_o-site is accompanied by dissociation of two protons, which finally appear in the aqueous bulk phase of the thylakoid lumen. According to the Q-cycle mechanism first suggested by Peter Mitchell (1976), the two-electron oxidation of PQH₂ in the Q_o-center is a bifurcated reaction (Berry et al. 2000; Crofts 2004a, b; Osyczka et al. 2004, 2005; Mulkidjianian 2005; Cramer et al. 2006, 2011; Crofts et al. 2013; Xia et al. 2013). One electron is directed from PQH₂ to a high-potential chain, the other electron travels along a low-potential chain (Fig. 10.3). The first electron comes to Pc through the high-potential redox chain, which consists of the ISP and Cyt *f* (PQH₂ → ISP → Cyt *f* → Pc). The second electron is directed to reduce PQ at the Q_i-site on the stromal side, traveling through the low- and high-potential hemes b₆^l and b₆^h: (PQH[•])_o → b₆^l → b₆^h → (PQ)_i. Here, (PQH[•])_o denotes the semiquinone form of plastoquinone formed upon the bifurcated oxidation of PQH₂ at the Q_o-site, (PQ)_i denotes the PQ molecule bound to the quinone-binding site Q_i located in the stromal part of the Cyt *b₆f* complex.

In the Q_i-center, after two successive steps of PQ reduction to PQ^{•-}, two protons are taken up from stroma (PQ + 2e⁻ + 2H_{out}⁺ → PQH₂). The protonated (electrically neutral) PQH₂ molecule dissociates from the Q_i-site and now it can bind to the vacant Q_o-site to be oxidized on the luminal side of the Cyt *b₆f* complex. Due to the round trip of one electron in the Q-cycle, the proton pumping activity of the Cyt *b₆f* complex increases by a factor of 2. Taking into account the overall balance of PQ turnover in the Q-cycle, we see that two hydrogen ions are pumped into the lumen per one electron (H⁺/e⁻ = 2) transferred from PQH₂ to P₇₀₀⁺ via the high-potential chain (ISP → Cyt *f* → Pc → P₇₀₀⁺). Note that the unique heme *c*₁ may be an adaptation of photosynthetic organisms for cyclic route of electron flow around PSI. Electrons from the acceptor side of PSI may return to the Q_i-center of the Cyt *b₆f* complex via Fd, FNR, and/or an atypical heme *c*₁ (Kurusu et al. 2003; Stroebel et al. 2003; Munekage et al. 2004; Joliot and Joliot 2005; Shikanai 2007).

10.2.3 The Cytochrome *b₆f* Complex and Alternative Pathways of Electron Transport

The Cyt *b₆f* complex is the participant of cyclic electron transport around PSI. On the acceptor side of PSI, apart from the mainstream pathway of electron flow to the CBC (the so-called “linear” electron flow, LEF), the electron flux may be diverted to cyclic routes around PSI. Cyclic electron flow around PSI (CEF1) is important for fine-tuning of the energy and redox balance in chloroplasts. There is general consensus that CEF1 helps to sustain the ratio ATP/NADPH = 3/2 required for optimal functioning of the CBC (for review, see Bendall and Manasse 1995; Allen 2003; Cruz et al. 2007; Johnson 2011; Strand et al. 2016). The light-induced transfer of four electrons from two H₂O molecules to two NADP⁺ molecules driven by the tandem operation of PSII and PSI (2H₂O + 2NADP⁺ → O₂ + 2NADPH) is

accompanied by pumping of 12 protons into the thylakoid lumen. This number of protons is insufficient for synthesis of three ATP molecules required to provide the ratio ATP/NADPH = 3/2. Actually, in chloroplasts the stoichiometric ratio $n = H^+ / ATP$ for the ATP synthase reaction ($ADP + P_i + nH_{in} \rightarrow ATP + nH_{out}$) is higher than $n = 4$ (Seelert et al. 2000; Junge and Nelson 2015; Turina et al. 2016). Therefore, 12 protons translocated inside the thylakoid per two NADPH molecules formed is insufficient to maintain the required ratio ATP/NADPH = 3/2. Additional pumping of protons coupled to operation of CEF1 could contribute to generation of Δm_{H^+} , providing synthesis of “extra” ATP molecules. Thus, the synergism of two pathways, LEF and CEF1, helps to maintain the ratio ATP/NADPH = 3/2 required for CO₂ fixation in the CBC. Even a relatively small contribution of CEF1 to generation of ΔpH may be enough to supplement ATP formation, providing thus the well-balanced ATP/NADPH ratio. CEF1 is also important for effective responses of PSA to fluctuations of light intensity, thereby avoiding the risk of photodamage to chloroplasts (Suorsa et al. 2012; Kono and Terashima 2014; Kono et al. 2014; Yamori and Shikanai 2016).

Most of CEF1 pathways involve the Cyt *b₆f* complex (Fig. 10.1). Recent genetic and biochemical studies clarified the physiological role of CEF1 and helped to elucidate the participation of different chloroplast proteins in CEF1 (for review, see Shikanai 2007). There are several routes of electron flow on the acceptor side of PSI, when electrons from PSI may be delivered to different channels (for recent review, see Strand et al. 2016). Electrons from PSI can be recycled to PQ from either reduced Fd (Fd⁻) or NADPH (“short” and “long” rounds, respectively). There are two “short” pathways of CEF1 related to electron transfer from Fd⁻ to PQ molecule bound to the Q_i-center mediated by the ferredoxin-plastoquinone-reductase (FQR) and FNR, without the participation of NADPH (pathways 1 and 2 depicted in Fig. 10.1). The “long” pathway of CEF1 involves the formation of NADPH and return of electrons through the chloroplast NAD(P)H-dehydrogenase (NDH): PSI → Fd → FNR → NADPH → NDH → PQ (Fig. 10.1, pathway 3).

One of the “short” routes of CEF1 implies the participation of the elusive FQR complex: PSI → Fd → FQR → PQ → *b₆f* (Bendall and Manasse 1995). It has been demonstrated that the products of two genes, *PGR5* (proton gradient regulation) and *PGRL1* (*PGR5*-like protein 1), may be involved into Fd-dependent CEF1 in eukaryotes (Munekage et al. 2002, 2004, 2008; Shikanai 2007; DalCorso et al. 2008; Suorsa et al. 2012; Hertle et al. 2013). Plants deficient in one of these proteins show disturbed CEF1, suggesting that *PGR5* and *PGRL1* may be considered as the components of FQR. The exact role of these proteins in CEF1 was unclear until it was demonstrated that *PGRL1* accepted electrons from Fd⁻ in a *PGR5*-dependent manner and reduced PQ (Hertle et al. 2013). These observations serve as compelling evidence that *PGRL1* operates as the elusive FQR protein. It is interesting to note that *PGRL1* is the redox regulated protein, its activity requires a Fe-containing cofactor and six redox-active cysteine residues. *PGR5* is used for electron transfer from Fd⁻ to *PGRL1*. Both proteins, *PGR5* and *PGRL1*, are necessary for PSA protection against photodamage induced by rapid fluctuations of ambient light (Munekage et al. 2008; Suorsa et al. 2012).

Another “short” route of Fd-dependent CEF1 implies the return of electrons from PSI to PQ through the FNR complex. The formation of a supercomplex FNR - *b₆f* (Zhang et al. 2001; Benz et al. 2010) may facilitate the direct electron transfer to the Q_i-site of the Cyt *b₆f* complex (Fig. 10.1, pathway 2). However, the nature of the immediate electron donor to PQ molecule at the Q_i-site is under debate (Shikanai 2007; DalCorso et al. 2008; Iwai et al. 2010; Johnson 2011). There are reasons to believe that an atypical heme *c*₁ positioned on the stromal side of the Cyt *b₆f* complex may serve as the immediate electron donor to PQ (Kurisu et al. 2003; Stroebel et al. 2003; Alric et al. 2005; Cramer et al. 2006, 2011; Hasan et al. 2013a). The PQ molecule bound to the Q_i-center may be reduced to PQH₂ by electrons coming from different chains. One electron comes from the high-potential heme *b₆^H*, whereas the second electron will arrive from PSI (Fig. 10.1, pathways 1 and 2). The reduced PQH₂ molecule dissociates from the Q_i-site and then can return to the Q_o-center, participating in the next cycle of PQH₂ turnover.

In the “long” (NADPH-dependent) route of CEF1, the NDH complex returns electrons from NADPH (and/or NADH) to the intersystem ETC (Fig. 10.1, pathway 3). Genetic and biochemical data give unequivocal evidence for participation of the chloroplast NDH in the “long” route of CEF1 (Burrows et al. 1998; Endo et al. 1998; Shikanai et al. 1998; Joët et al. 2001; Shikanai 2016). There are indications that the NDH and PSI complexes can form a supercomplex (NDH-PSI) in higher plants (Peng et al. 2008, 2009) and cyanobacteria (Kubota et al. 2009). The location of NDH in the stromal lamellae close to PSI as well as an elevated content of NDH in the bundle sheath cells of C₄ plants with high levels of CEF1 (Kubicki et al. 1996) support the notion of NDH participation in CEF1.

10.2.4 Lateral Heterogeneity of Thylakoid Membranes

The participation of the Cyt *b₆f* complex in CEF1 depends on its location in the thylakoid membrane. The arrangement of membrane-embedded electron transport complexes and mobile electron carriers with respect to stromal and granal thylakoids is shown schematically in Fig. 10.4. It is well-known fact that PSI, PSII, and ATP synthase (CF₀ - CF₁) complexes are distributed nonuniformly over the membranes of granal and stromal thylakoids (Albertsson 2001; Staehelin 2003; Dekker and Boekema 2005). Stacked thylakoids of grana are enriched with PSII; most PSI and CF₀ - CF₁ complexes are localized in the unstacked domains of stroma-exposed thylakoids, grana margins, and grana end membranes. The Cyt *b₆f* complexes are spread almost uniformly along the thylakoid membranes (Anderson 1982). About 55% of the Cyt *b₆f* complexes are localized in appressed membranes of grana, and about 45% of complexes are distributed over the stromal lamellae, in the margins and grana end membranes. Although significant amounts of PSI, PSII, and Cyt *b₆f* complexes are laterally segregated in the thylakoid membrane, most of them are in close contact. The content of different electron-transport complexes and their ratio (PSII/*b₆f*/PSI) are variable, being sensitive to the plant growth conditions (for

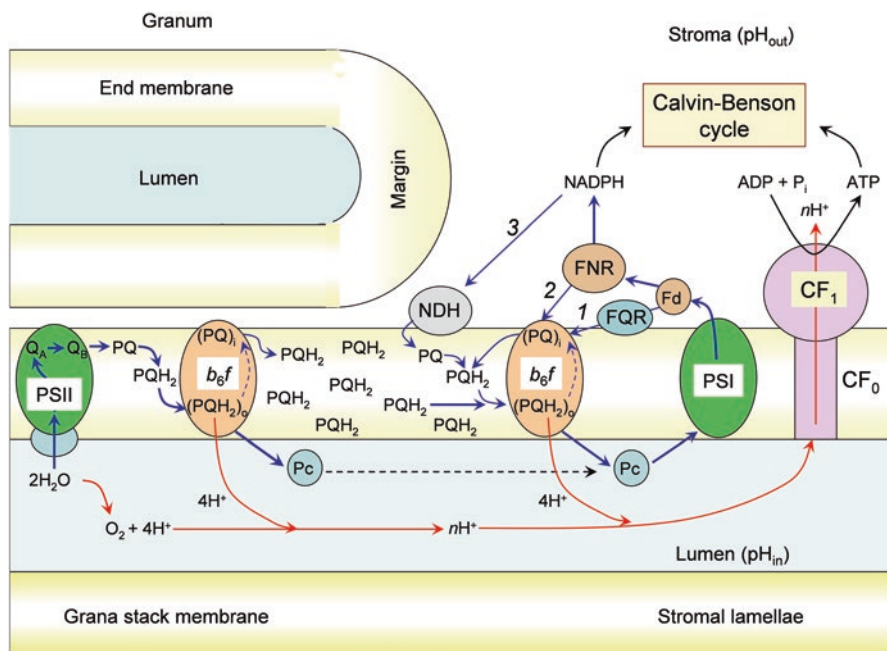


Fig. 10.4 A scheme of the possible arrangement of the electron transport and ATP synthase complexes in the stromal and granal domains of the thylakoid membrane (Modified from Figure 4 in Tikhonov 2014)

review, see Anderson et al. 1988; Lichtenthaler and Babani 2004; Eberhard et al. 2008; Schöttler et al. 2015; Puthiyaveetil et al. 2016). The amounts of PQ and Pc are higher than that of PSI or PSII. The relative capacity of the PQ pool, related to PSII, was estimated as PQ/PSII ~ 10 times (Stiehl and Witt 1969; Witt 1979; Haehnel 1984).

It is important to note that there are two population of the Cyt *b₆f* complex, that differ from each other with respect to their location in the stromal and granal domains of thylakoid membranes. Under the normal physiological conditions, grana-exposed thylakoids are assembled in the form of grana consisting of tightly packed thylakoid disks. Because of steric restrictions, direct contacts of granal Cyt *b₆f* complexes with the FNR complexes will be excluded. This circumstance suggests that only the stroma-exposed fraction of Cyt *b₆f* complexes may participate in the CEF1 reactions (Joliot and Joliot 2005, 2006). Although significant amounts of PSI and PSII complexes are laterally segregated, most of them are in close contact with the Cyt *b₆f* complexes (Albertsson 2001). The proximal location of the Cyt *b₆f* complexes to PSII in granal domains of thylakoid membranes should facilitate electron transfer between PSII and the Cyt *b₆f* complexes due to a short distance for PQH₂ diffusion in the lipid phase of the membrane (Kirchhoff 2013, 2014). This circumstance may shed a light on the nature of the rate-limiting step in the intersystem chain of electron transport, considered below.

10.2.5 *The Rate-Limiting Step in the Intersystem Chain of Electron Transport*

The rate of PQ turnover is determined by several events: PQ reduction to PQH₂ ($\text{PQ}_B + 2e^- + 2\text{H}_{\text{out}}^+ \rightarrow \text{PQ}_B\text{H}_2$), dissociation of PQH₂ from PSII, its diffusion towards the Cyt *b₆f* complex, and oxidation of PQH₂ at the Q_o-site. The peculiarities of chloroplast architecture raise the question as to whether or not the lateral and transverse diffusion of PQH₂ molecules within the thylakoid membrane would restrict the intersystem electron transfer. Which stage of PQH₂ oxidation determines the rate of PQH₂ turnover, either the lateral diffusion of PQH₂ in the membrane between spatially separated electron transport complexes or PQH₂ oxidation after its binding to the Cyt *b₆f* complex? There are indications that the lateral diffusion of PQH₂ may restrain electron transfer from PSII to PSI under certain conditions (Lavergne and Joliot 1991; Kirchhoff 2008, 2014). Diffusion of PQH₂ within the membrane may be retarded due to obstructed diffusion of PQH₂ through the lipid domains, over-crowded with densely packed protein complexes. In the meantime, as noted above, the distribution of Cyt *b₆f* complexes among PSII complexes located in granal thylakoids minimizes the average distance traversed by PQ molecules, providing rapid turnover of the PQ shuttle between the Cyt *b₆f* and PSII complexes.

In earlier work (Stiehl and Witt 1969), these authors scrutinized in detail the PQ turnover in spinach chloroplasts by optical methods. Redox transients of PQH₂ were measured by monitoring absorption changes in the UV region. It was demonstrated that PQH₂ delivered electrons to P₇₀₀⁺ (via intermediates) with the half-time $t_{1/2} \approx 15 - 17.5$ ms. Similar times were obtained by Haehnel for Cyt *f* and P₇₀₀⁺ reduction (Haehnel 1973, 1976a, b). Electron transfer from the Cyt *b₆f* complex to P₇₀₀⁺ occurred much more rapidly than PQH₂ oxidation: $t_{1/2} \approx 35 - 350$ μs for electron transfer from Cyt *f* to Pc, and $t_{1/2} \approx 20 - 200$ μs for electron transfer from Pc to P₇₀₀⁺ (Haehnel 1984; Hope 2000). These results unequivocally demonstrated that PQH₂ interaction with the Cyt *b₆f* complex to be the rate-limiting event in the chain of electron transport processes between PSII and PSI.

There is strong evidence that within a wide range of experimental conditions (pH, ionic strength, and temperature) PQH₂ formation and its diffusion in the membrane do not limit the intersystem electron transport. The light-induced reduction of PQ in PSII ($\text{PQ}_B + 2e^- + 2\text{H}_{\text{out}}^+ \rightarrow \text{PQ}_B\text{H}_2$), dissociation of PQ_BH₂ from PSII ($\text{PQ}_B\text{H}_2 \rightarrow \text{PQH}_2$) and PQH₂ diffusion to the Cyt *b₆f* complex occur more rapidly than PQH₂ interaction with the Cyt *b₆f* complex (Haehnel 1976a; Tikhonov et al. 1984). This statement can be illustrated by the experimental data presented in Fig. 10.5. In chloroplasts pre-illuminated with the far-red light ($\lambda_{\text{max}} = 707$ nm) exciting predominantly PSI, the PQ pool and most of P₇₀₀ centers become oxidized because of negligible injection of electrons from PSII to the intersystem ETC. In response to a short flash of white light exciting both photosystems, electrons donated by PSII are used to reduce oxidized centers P₇₀₀⁺ (Fig. 10.5a). In the particular case of Mg²⁺-depleted chloroplasts, the reduction of P₇₀₀⁺ proceeds after a well-resolved

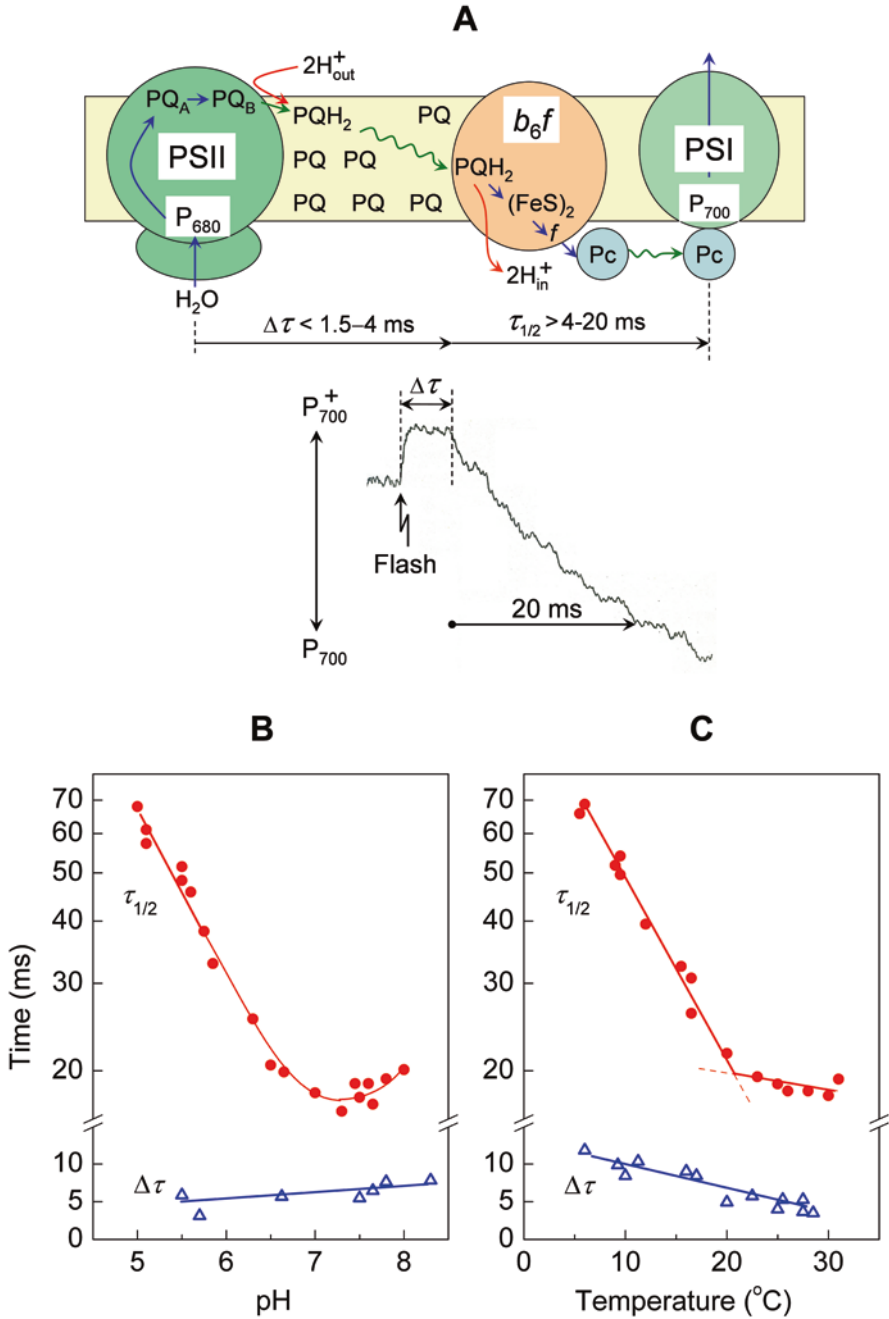


Fig. 10.5 Panel A shows the kinetics of P_{700} redox transients induced by a short pulse ($t_{1/2} = 7 \mu s$) of white light given on the background of a continuous far-red light ($\lambda_{max} = 707$ nm). Panels B and C illustrate the influence of pH and temperature on kinetic parameters Δt and $\tau_{1/2}$ for P_{700} transients (see panel A for definition) (Modified figures adopted from Tikhonov (2014, panel A) and Tikhonov et al. (1984, panels B and C))

lag-phase, the duration of which ($\Delta\tau$) involves the time of PQH₂ formation and diffusion across and along the thylakoid membrane towards the Cyt *b₆f* complex. The half-time of P₇₀₀⁺ reduction, which is determined mainly by electron transfer from PQH₂ bound to the Cyt *b₆f* complex, is markedly higher than the lag-phase $\Delta\tau$ (Fig. 10.5a). This observation demonstrates that PQH₂ oxidation at the Q_o-site of the Cyt *b₆f* complex represents the “bottle-neck” in the ETC between PSII and PSI, which controls the overall rate of the intersystem electron transport. Actually, the interaction of Pc⁻ with P₇₀₀⁺ usually occurs much more rapidly ($t_{1/2} \leq 200 \mu\text{s}$, at ambient temperatures) than electron transfer from PQH₂ to Pc via the Cyt *b₆f* complex (Stiehl and Witt 1969; Witt 1979; Haehnel 1984). The duration of the lag-phase $\Delta\tau$ is sensitive to Mg²⁺-induced structural changes in chloroplasts. At physiological concentrations of MgCl₂ (2–4 mM), $\Delta\tau$ is significantly shorter than in Mg²⁺-depleted chloroplasts, although the addition of MgCl₂ had no marked effect on $\tau_{1/2}$ (Tikhonov et al. 1984). Since the lag-phase $\Delta\tau$ is always shorter ($\Delta\tau \leq 4 \text{ ms}$) than the half-time of P₇₀₀⁺ reduction ($t_{1/2} \approx 18 - 20 \text{ ms}$), one can conclude that the formation of PQH₂ and its diffusion to the Cyt *b₆f* complex occur more rapidly than PQH₂ oxidation at the Q_o-site.

A significant difference between kinetic parameters $\Delta\tau$ and $\tau_{1/2}$ was observed over a wide range of pH (Fig. 10.5b) and temperature (Fig. 10.5c). These observations provide clear evidence that the overall rate of the intersystem electron transfer is determined mainly by PQH₂ oxidation at the Q_o-site, a rate that decelerates with the lumen acidification and a decrease in temperature. Short times of PQH₂ diffusion from PSII to the Cyt *b₆f* complex may be accounted for, at least partly, by the close neighbourhood of these complexes in the granal domains of the thylakoid membrane. Note that the temperature dependence of P₇₀₀⁺ reduction in isolated bean chloroplasts reveals the characteristic “break” at $\approx 20^\circ\text{C}$. Below this temperature ($\leq 20^\circ\text{C}$), kinetic parameter $\tau_{1/2}$ (the half-time of P₇₀₀⁺ reduction) strongly depends on the temperature; at higher temperatures ($\geq 20^\circ\text{C}$), $\tau_{1/2}$ is almost independent of temperature. As it was demonstrated in earlier works (Tikhonov et al. 1980, 1983), this peculiarity of the temperature dependence of $\tau_{1/2}$ (as well as the rate of ATP synthesis) strongly correlates with thermo-induced structural changes detected in the lipid phase of the thylakoid membrane with the lipid-soluble spin-probes (nitroxide radicals). One can speculate, therefore, that thermoinduced changes in the lipid phase of the thylakoid membrane can affect the rate of PQ turnover. For instance, “solidification” of the lipid bilayer with lowering the temperature may reduce the rate of the PQH₂ - *b₆f* complex formation, and/or would cause the slowing down of PQH₂ oxidation due to decelerated release of protons into the lumen, which is considered as the prerequisite for PQH₂ oxidation by the Cyt *b₆f* complex.

The notion that a relatively high mobility of PQH₂ in the thylakoid membrane finds support from computer simulation of PQ diffusion, suggests that PQH₂ could travel farther than 290 nm in 10 ms (Tremmel et al. 2003). This estimate is in agreement with experimental data, demonstrating that electron transfer between PSII to PSI is not limited by PQH₂ migration along the thylakoid membrane. High rates of PQH₂ diffusion in the thylakoid membrane suggest that the rate of PQ turnover in

chloroplasts is determined predominantly by the events associated with the PQH₂ penetration to the Q_o-cavity and its oxidation within the Cyt b_6f complex (for review, see Tikhonov 2013, 2014).

Summing up the above reasonings, one can conclude that the light-induced reduction of PQ to PQH₂ in PSII occurs much more rapidly than PQH₂ oxidation by the Cyt b_6f complex. It is noteworthy, however, that experimental data for partial reactions of electron transfer within the Cyt b_6f complex are often scattered, depending on the system investigated and its metabolic state. For instance, the post-illumination reduction of Cyt f in different species of intact leaves was characterized by half-times ranging from 20 to 28 ms for a wide range of light intensities (up to 2800 of photons $\mu\text{mol m}^{-2}\text{s}^{-1}$, Kramer et al. 1999). Alternatively, several authors reported a more rapid turnover of the Cyt b_6f complex in leaves (Harbinson and Hedley 1989; Laisk et al. 2005). Relatively short apparent times of Cyt f and Cyt b reduction ($t_{1/2} \approx 3 - 6$ ms) are typical of intact *C. reinhardtii* cells (Soriano et al. 1996; Ponamarev and Cramer 1998) and the cyanobacterium *Synechococcus* sp. PCC 7002 (Yan and Cramer 2003). Dispersion of kinetic data might be explained by several reasons, e.g., due to differences between the species and variable stoichiometry between PSII, Cyt b_6f , and PSI complexes (Schöttler et al. 2015; Puthiyaveetil et al. 2016). Variability of electron capacities of redox partners on the donor and acceptor sides of the Cyt b_6f complex may also influence the kinetic behaviour of the system, exaggerating or underestimating the contributions of rapid and slow phases of electron transport processes (for recent discussion of this point, see Tikhonov 2016). Nevertheless, the rate of PQH₂ oxidation in the Cyt b_6f complex comprises the rate-limiting step in the chain of electron transport between PSII and PSI.

Let us now consider another aspect of PQH₂ interaction with the Cyt b_6f complex related to variability of the rates of PQH₂ oxidation and P₇₀₀⁺ reduction. Speaking of kinetic peculiarities of PQH₂ interaction with the Cyt b_6f complex, one has to take into account connectivity between spatially separated electron transport complexes via the mobile electron carriers, PQ and Pc (this scenario is depicted symbolically in Fig. 10.6a). Spatially separated PSII and Cyt b_6f complexes can interact with each other due to rapid diffusion of PQH₂ and PQ molecules within the thylakoid membrane and fast diffusion of Pc molecules in the lumen. An apparent rate of electron transfer from PQH₂ to PSI is sensitive to the redox status of the ETC. With the rise of PQH₂ concentration, the probability of formation of the substrate-enzyme complex PQH₂ - b_6f increases, thereby accelerating the overall rate of electron flow from PSII to P₇₀₀⁺. This point can be illustrated by the data presented in Fig. 10.6b, which shows that the initial rate of P₇₀₀⁺ reduction ($R_{P_{700}^+}$) in response to light pulses of various duration increases with the rise of a number of electrons per P₇₀₀ (N_e) injected from PSII into the intersystem ETC (Tikhonov et al. 1980). Saturation of kinetic parameter $R_{P_{700}^+}$ at sufficiently high numbers of electrons injected ($N_e > 2$) implies that the proton-coupled electron transfer (PCET) events, taking place within the Cyt b_6f complex after PQH₂ binding to the Q_o-center, determine the rate of PQH₂ turnover. A similar result was reported by Haehnel (1973) who observed acceleration of P₇₀₀⁺ reduction with an increase in the number of consecutive light flashes illuminating spinach chloroplasts. Analysis of experimental data on the redox

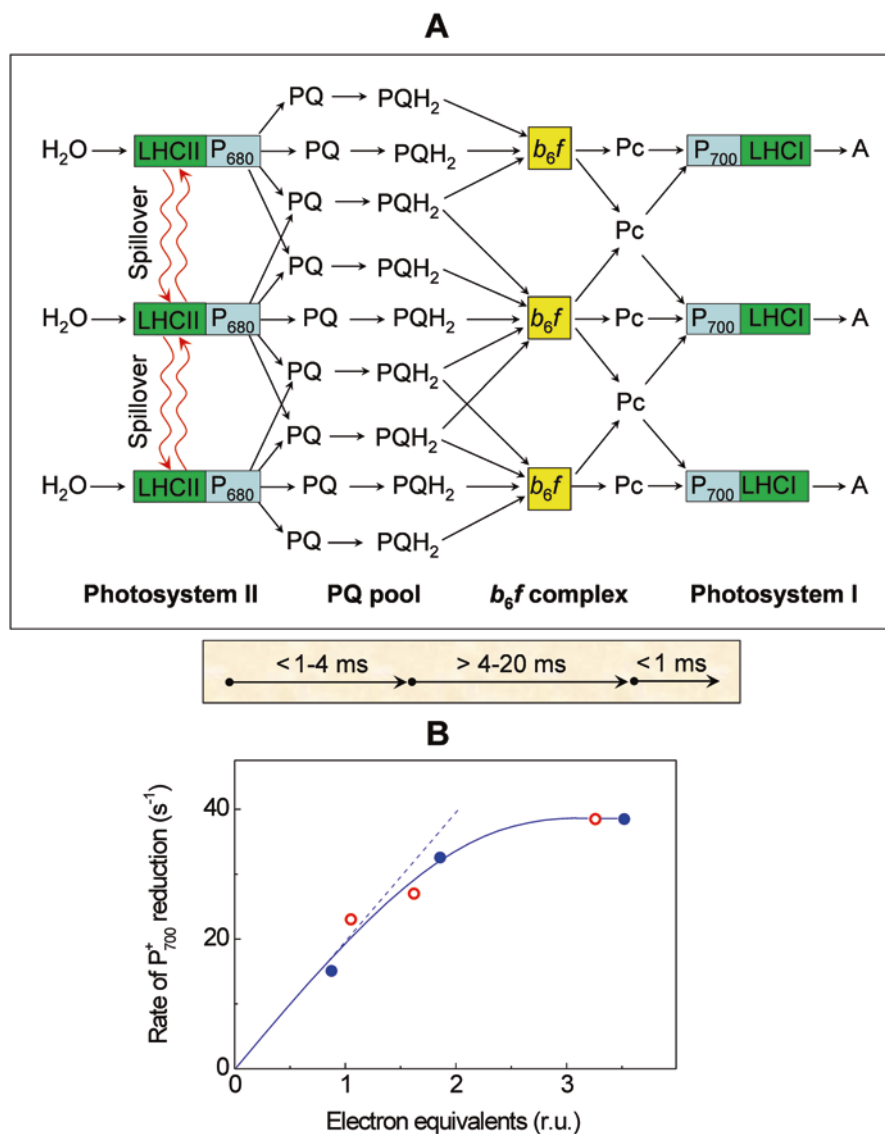


Fig. 10.6 Panel **A** illustrates the connectivity between different electron transport complexes by means of mobile electron carriers, plastoquinone (PQ) and plastocyanin (Pc); ripple-type arrows (termed “spillover”) symbolize the excitonic mechanism of interaction between the light harvesting complexes of PSII (LHCII), after (Tikhonov and Vershubskii 2017). Panel **B** shows the dependence of the initial rate of post-illumination reduction of P_{700}^+ in bean chloroplasts *versus* an average number of electrons (per P_{700}) injected into the intersystem electron transport chain in response to light pulses of different duration. Kinetic data used in plot **B** were compiled from Figs. 7 and 8 presented in (Tikhonov et al. 1980). Open and closed circles correspond to measurements at 20 °C and 29 °C, respectively

transients of P_{700} within the framework of a mathematical model also suggests that even significant attenuation of PSII activity (for instance, due to generation of NPQ) may not cause drastic reduction of electron flow through PSI during the action of a sufficiently strong continuous actinic light (Tikhonov and Vershubskii 2017). This result can be explained by “electronic” and/or “excitonic” connectivity between different PSII units (Siggel et al. 1972; Tikhonov and Ruuge 1979; Haehnel 1982; Stirbet 2013). At sufficiently strong actinic light, the overall flux of electrons between PSII and PSI would maintain at a high level even upon the attenuation of PSII activity, provided the rate-limiting step of electron transfer is beyond the stage of PQH₂ formation (Tikhonov and Vershubskii 2017). This is because the PQH₂ pool serves as the redox buffer, which can accumulate electron equivalents capable of reducing P_{700}^+ via the Cyt *b₆f* complex and Pc.

10.3 Plastoquinol Interaction with the Cytochrome *b₆f* Complex

10.3.1 *Q*-Cycle

Oxidation of PQH₂ occurs after its penetration into the quinone-exchange cavity and binding to the Q_o-center positioned on the luminal side of the Cyt *b₆f* complex. One can say that two reagents, PQH₂ and oxidized ISP (ISP_{ox}), form the “enzyme-substrate” complex (ES-complex). According to the earlier models of quinol oxidation, electron transfer from the quinol molecule to the ISP_{ox} proceeds only after the quinol deprotonation reaction (QH₂ → QH⁻ + H⁺).¹ The “proton-gated affinity change” (Link 1997) and the “proton-gated charge transfer” (Brandt 1996; Brandt and Okun 1997) mechanisms imply that it is the anion form of the quinol (QH⁻) that binds to the Q_o-center and then donates electron donor to oxidized redox center of the Rieske protein (ISP_{ox}). Crofts and collaborators suggested that the formation of the ES-complex does not need the dissociation of a proton from QH₂, but involves the dissociated form of the ISP_{ox} (Crofts 2004a, b; Crofts et al. 2013). The ES-complex QH₂ - ISP_{ox} is stabilized by the hydrogen bond between the -OH group of the quinol molecule and the imidazolate ring of deprotonated ISP_{ox} (Fig. 10.7). The redox center of the ISP contains the [Fe₂S₂] cluster, one of the Fe atoms of which is ligated by two His residues (His136 and His155 in *C. reinhardtii*). In the oxidized state, this cluster is diamagnetic (spin $S = 0$) due to the antiferromagnetic coupling between two Fe³⁺ ions. In the reduced state, the [Fe₂S₂] cluster becomes paramagnetic (spin $S = 1/2$) and, therefore, it can be detected by the electron paramagnetic resonance method at cryogenic temperatures (Zhang et al. 1996; Soriano et al. 2002).

¹Here and below, the general terms QH₂ and Q are used to denote the quinol and quinone species, regardless of their origin (plastoquinone, PQ, or ubiquinone, UQ). SQ designates the redox states of semiquinone species, either plastosemiquinone (in the *b₆f* complex) or ubisemiquinone (in the *bc₁* complex), regardless of their protonation state.

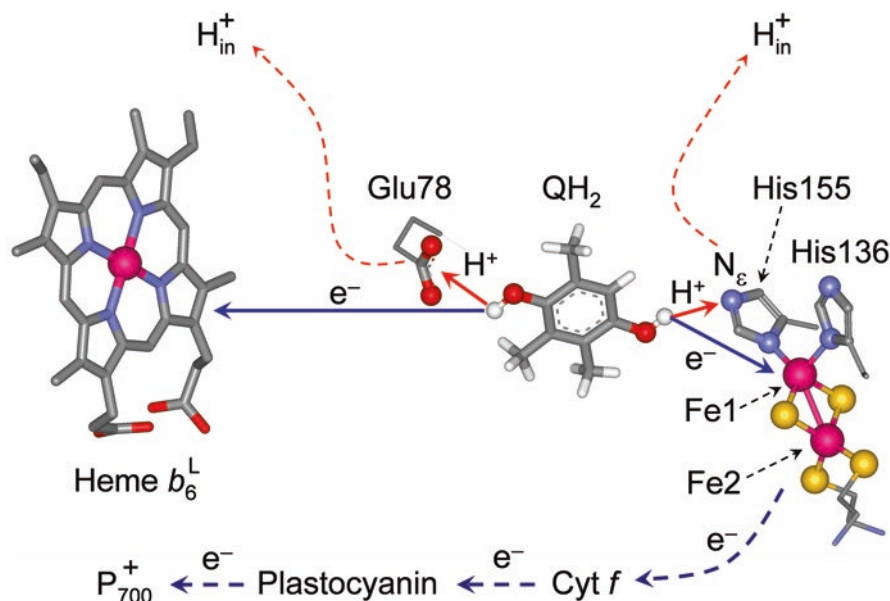


Fig. 10.7 Schematic representation of electron and proton transfer reactions upon the two-electron oxidation of quinol at the Q_o-site of the Cyt b₆f complex from *Chlamydomonas reinhardtii* (PDB entry 1Q90, Stroebel et al. 2003). Figure was produced using Accelrys DV visualizer software package (<http://www.accelrys.com>)

The bifurcated reaction of PQH₂ oxidation proceeds as two *concerted* reactions of *proton-coupled* electron transfer (PCET): (i) PQH₂ → SQ + e⁻ + H⁺, and (ii) SQ → PQ + e⁻ + H⁺, where SQ denotes the semiquinone form of PQ or ubiquinone (UQ) (Berry et al. 2000; Cramer et al. 2006, 2011; Hasan et al. 2013a; Crofts 2004a, b; Crofts et al. 2013; Snyder et al. 2000; Cape et al. 2007). The term “proton-coupled” means that reactions (i) and (ii) are tightly coupled to proton transfer from PQH₂ and SQ to appropriate proton-accepting groups, respectively. The term “concerted” implies that both reactions (i) and (ii) occur simultaneously (or almost simultaneously) (Osyczka et al. 2004, 2005; Zhu et al. 2007).

Plastoquinol Oxidation Reactions The pictorial scheme of events associated with the bifurcated (two-electron) oxidation of PQH₂ within the framework of the Mitchellian Q-cycle is shown in Fig. 10.8. The turnover of PQH₂ molecules in the Q_o-center starts with the first reaction of electron transfer. Oxidized iron-sulfur cluster of the ISP (ISP_{ox}⁺) serves as the primary electron acceptor in the high-potential redox chain reduced by PQH₂:



This reaction is the PCET process, in which the electron and proton transfer proceed as tightly coupled events. Structural data suggest that the N_ε atom of the histidine residue, which ligates the [Fe₂S₂] cluster of the ISP extrinsic domain of the Cyt b₆f

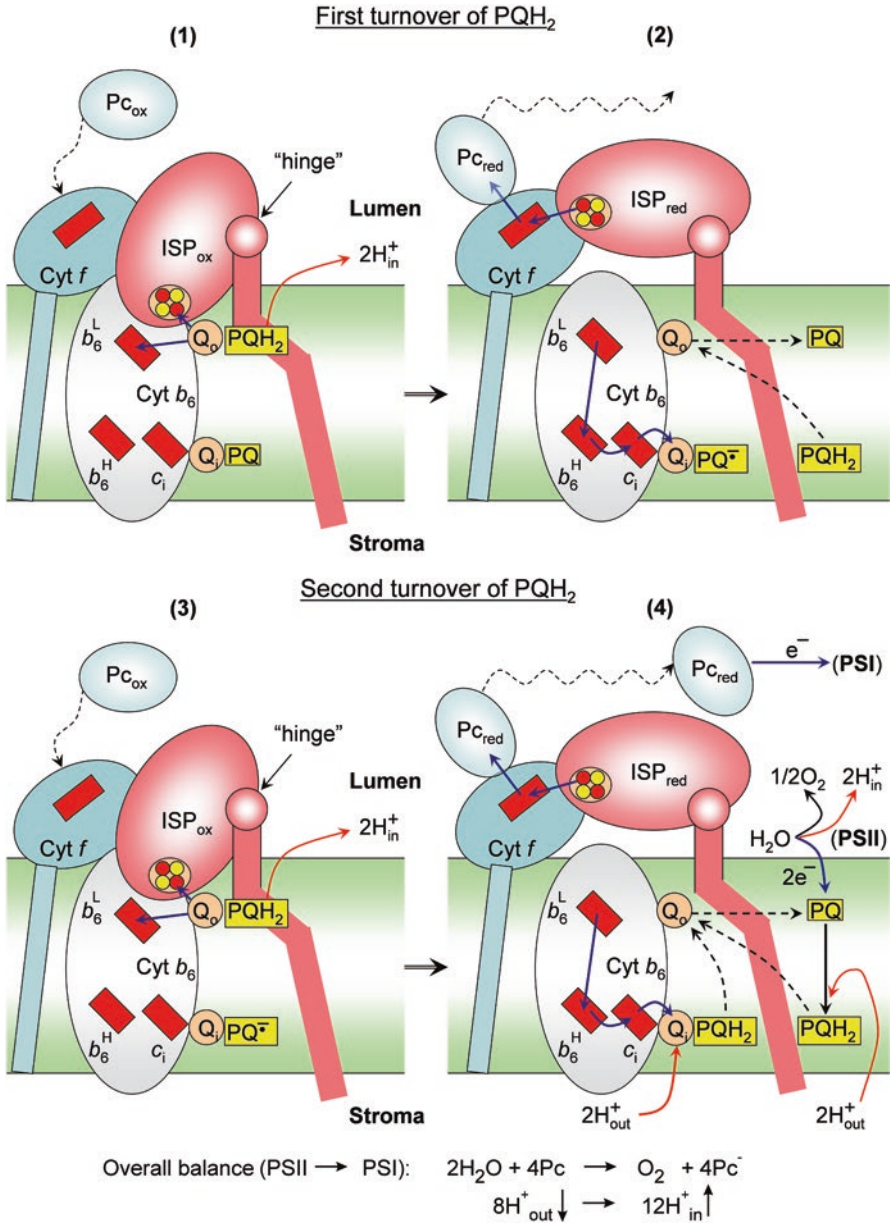


Fig. 10.8 A sketch illustrating plastoquinone turnover in the Cyt *b₆f* complex within the framework of the Q-cycle model

complex (His155 in *C. reinhardtii* or His129 in *M. laminosus*), is the prime candidate for the role of the recipient accepting the proton from PQH₂ (Fig. 10.7). This residue of the ISP is within hydrogen-bonding distance from the –OH group of the quinol. The formation of the hydrogen bond between this group and the N_ε atom of the neighboring histidine is considered as an essential prerequisite for the first reaction (10.1) of quinol oxidation (Hsueh et al. 2010; Lhee et al. 2010). The notion about the formation of such a hydrogen bond finds strong support from spectroscopic (EPR, NMR, and ATR-FTIR) studies of the *bc*₁ complex (Samoilova et al. 2002; Zu et al. 2003; Iwaki et al. 2005; Lin et al. 2006; Hsueh et al. 2010; Lhee et al. 2010), which is akin to the *b₆f* complex.

The plastoquinone molecule formed as the result of the first PCET reaction (10.1) will be in the neutral form (PQH[•]). In the second PCET reaction (10.2), PQH[•] donates an electron to the low-potential heme *b₆^L* of the low-potential branch of the Cyt *b₆f* complex:



In chloroplasts, the key role in the proton migration from PQH[•] to the lumen belongs to the proton-accepting carboxyl group of glutamate (Glu78). Glu 78 is part of a highly conserved PEWY sequence of subunit IV, which participates in the formation of the quinone-binding pocket of the Q_o-center. The proton-accepting group of Glu78 is positioned between the PQH₂ molecule and heme *b₆^L* (Fig. 10.7). This group may serve as the primary recipient of the proton from PQH[•] (Zito et al. 1998). It has been suggested, on the basis of structural and mutagenesis data for the Cyt *bc*₁ complex, that Glu in the PEWY-span accepts a proton from the neutral semiquinone, and delivers it by rotation of the carboxylic side chain to the proton exit channel, leaving the anionic form of SQ in the Q_o-site (Victoria et al. 2013). Mutagenesis of Glu78 is known to impair turnover of the Cyt *b₆f* complex in *C. reinhardtii* (Zito et al. 1998; Finazzi 2002). A similar effect of the impediment to UQH₂ oxidation has been described for the Cyt *bc*₁ complex (Victoria et al. 2013). The proton from the carboxyl group of Glu78 migrates to the lumen through one of putative proton-conducting pathways (Hasan et al. 2013c; Tikhonov 2014).

The reduced ISP_{red} passes an electron to heme *f* located in the peripheral domain of the Cyt *f* protein. The ISP occupies a cleft between the large and small domains of Cyt *f* (Fig. 10.3). A key step of electron transfer from the [Fe₂S₂] cluster of the ISP to the Cyt *f* heme involves the large-scale conformational changes within the Cyt *b₆f* complex. A distance between the redox cluster [Fe₂S₂] docked nearby the Q_o-center and heme *f* is too long (≈ 26 Å) in order to provide physiologically rapid direct transfer of electrons from the ISP_{red} to Cyt *f* by the mechanism of quantum mechanical tunneling (Page et al. 1999). However, a high mobility of the extrinsic domain of the ISP containing the redox cluster [Fe₂S₂] should facilitate electron transfer between the ISP_{red} and oxidized Cyt *f*. It is likely that after the reduction of ISP its extrinsic domain moves from the proximal position in the vicinity of the Q_o-site towards the distal position close to the heme *f*, thereby providing electron

transfer from the ISP_{red} to Cyt *f*. This case is cartooned as the transition from the state (1) to state (2) shown in Fig. 10.8.

There are several lines of evidence for a high mobility of the extrinsic domain of the ISP containing the redox center $[\text{Fe}_2\text{S}_2]$ within the whole ensemble of the Cyt *b₆f* complex (Breyton 2000; Heimann et al. 2000; Soriano et al. 2002; Roberts et al. 2002; Yan and Cramer 2003; de Vitry et al. 2004). One of the convincing arguments in favor of the cluster $[\text{Fe}_2\text{S}_2]$ mobility, which paves the way for electronic communication between the ISP and Cyt *f*, may be considered from the results of the X-ray data on the Cyt *b₆f* complex from *M. laminosus* (Hasan et al. 2013b). This conclusion stems from extensive crystallographic disorder of the ISP extrinsic domain indicating its conformational flexibility. The ISP disorder has been observed in the Cyt *b₆f* complex supplemented with anionic lipids. This indicated that the electric charges on the lipid headgroups may influence motion of the ISP extrinsic domain within the Cyt *b₆f* complex. Structural data first obtained for a variety of Cyt *bc₁* complexes of different origin present the apt evidence for the long-range movements of the flexible domain of the ISP containing the Rieske $[\text{Fe}_2\text{S}_2]$ cluster (for review, see Darrouzet et al. 2001; Xia et al. 2013). Two different positions of the $[\text{Fe}_2\text{S}_2]$ cluster relative to heme *c₁* have been found in the X-ray crystallographic structures in the presence or absence of various inhibitors, suggesting the large-scale movement of the extrinsic domain of the ISP containing the $[\text{Fe}_2\text{S}_2]$ cluster (Iwata et al. 1998; Kim et al. 1998; Zhang et al. 1998; Esser et al. 2006).

The long-range “tethered” diffusion of the $[\text{Fe}_2\text{S}_2]$ cluster towards heme *f* enables electron transfer from ISP_{red} to Cyt *f* and further to plastocyanin. After oxidation and deprotonation of the ISP_{red} ($\text{ISP}_{\text{red}}^{\cdot-} + \text{H}^+ + f \rightarrow \text{ISP}_{\text{ox}} + f^- + \text{H}_{\text{in}}^+$), its mobile extrinsic domain returns from the distant (Fig. 10.8, panel 2) to the proximal position near the Q_o -site (Fig. 10.8, panel 3). Note that the movements of the ISP extrinsic domain between the proximal (Q_o -site) and distal positions (heme *f* in the Cyt *b₆f* complex or heme *c₁* in the Cyt *bc₁* complex) are more rapid than the overall process of quinol oxidation. A mutagenesis study of the ISP in *C. reinhardtii* (de Vitry et al. 2004) indicated that the protein-linking domain of the chloroplast ISP was much more flexible than its counterpart in mitochondria. This was explained by the greater flexibility of the polyglycine hinge in the Cyt *b₆f* complex than of the polyalanine hinge in the Cyt *bc₁* complex (Yan and Cramer 2003).

The destiny of the second electron donated by PQH_2 differs from that of the first electron. After the removal of the first electron and proton from PQH_2 in the Q_o -center (the first PCET reaction), the extrinsic domain of the ISP moves towards heme *f*. Displacement of the redox center $[\text{Fe}_2\text{S}_2]$ away from the Q_o -site precludes the thermodynamically favorable donation of the second electron from SQ to the high-potential branch, directing the SQ radical to reduce the low-potential heme b_6^{L} . After electron transfer from the plastosemiquinone PQH^{\cdot} to the low-potential heme b_6^{L} (reaction 2), the electron is transferred to the high-potential heme b_6^{H} and further to heme *c₁*, towards the PQ binding site Q_i on the stromal side of the Cyt *b₆f* complex, reducing $(\text{PQ})_i$ to its plastosemiquinone anion-radical species $(\text{PQ}^{\cdot-})_i$.

(Fig. 10.8, panel 2).² After the second turn of PQH₂ turnover, PQH₂ forms in the Q_i-center, $(PQ^{\bullet})_i + e^- + 2H_{out}^+ \rightarrow (PQH_2)_i$, and then dissociates into the membrane (Fig. 10.8, panels 3 and 4).

Taking into account that two protons appear in the lumen per one H₂O molecule oxidized in the WOC of PSII ($H^+/e^- = 1$) and four protons are pumped into the lumen per two electrons transferred to PSI through the Cyt *b₆f* complex ($H^+/e^- = 2$), the overall stoichiometry of proton and electron transport is $H^+/e^- = 3$. This means that three hydrogen ions will appear into the lumen per one electron transferred from PSII to PSI. Thus, the operation of the Q-cycle enhances the proton/electron stoichiometry, increasing the efficiency of proton pumping into the lumen, as was first predicted by Peter Mitchell who put forward his brilliant idea of the Q-cycle as early as 1976 (Mitchell 1976). It is note worthy to stress that two-thirds of the *trans*-thylakoid pH difference (Δ pH) in oxygenic photosynthesis originates from the proton pumping by the Cyt *b₆f* complex.

Proton Exit Pathways Oxidation of PQH₂ occurs as the proton-coupled reactions, in which two protons migrate into the aqueous bulk phase of the lumen. Each of two steps of the PQH₂ oxidation reaction is accompanied by deprotonation. Analysis of the crystal structure of the Cyt *b₆f* complex from *C. reinhardtii* (PDB entry 1Q90) revealed two putative pathways for proton release from the PQH₂ molecule oxidized at the Q_o-site (Fig. 10.9). The side residue of His ligating the [Fe₂S₂] cluster of the ISP (His155 in *C. reinhardtii*, or His129 in *M. laminosus*) may serve the role of the immediate recipient of the first proton donated by PQH₂. Being bound to this His residue of the extrinsic domain of ISP, the proton extracted from PQH₂ starts traveling along the exit route to the aqueous bulk phase of the lumen. After oxidation of protonated ISP_{red} by Cyt *f* ($ISP_{red}^+ H^+ + f \rightarrow ISP_{ox} + f^- + H_{in}^+$) its affinity for a proton decreases and the proton releases from the ISP, migrating to the lumen through the *intra*-protein proton-conducting channel containing water molecules. The structural and biochemical data indicate that the water molecules of the proton-conductive chain, in addition to the surrounding amino acid residues, play an important role in Cyt *f* functioning (Ponamarev and Cramer 1998; Sainz et al. 2000). Interruption of the internal water chain, which forms a path for proton migration, impairs the operation of the Cyt *b₆f* complex: electron transport from the ISP to Cyt *f* decelerates, and the concerted reduction of Cyt *b₆* and Cyt *f* is lost. An alternative point of view on the nature of the primary recipient of the proton donated by quinol has been suggested by Postila et al. (2013), who scrutinized the problem on the basis of atomic molecular dynamics simulations for the Cyt *bc₁* complex. They suggested that water molecules positioned in suitable places of the Q_o-site nearby the UQH₂ molecule could act as the primary proton-receiving partners in the two-electron oxidation of UQH₂.

²It is likely that this species will appear in the form of the anion-radical $PQ^{\bullet-}$, because the pK values of semiquinones are usually fall in the range below the stromal pH establishes under the normal physiological conditions ($pH_{out} \sim 7 - 8$).

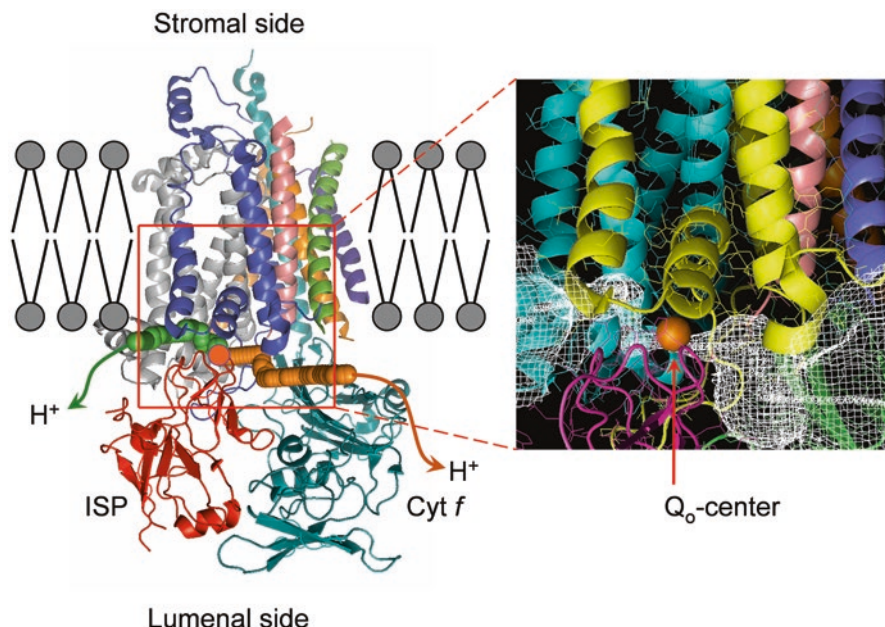


Fig. 10.9 Side view of the monomeric fragment the Cyt *b₆f* complex from *Chlamydomonas reinhardtii* (PDB entry 1Q90, Stroebel et al. 2003), which demonstrate putative exit pathways for protons dissociating from the Q_o -site to the thylakoid lumen. The traces of the proton-conducting pathways (shown by green and brown spheres) were found in collaboration with B.V.Trubitsin, using the program Cover for detection of possible channels for traveling mobile molecules inside protein structures (Chovancová et al. 2012). The program output was visualized using PyMOL Molecular Graphics System

Oxidation of semiquinone PQH^{\bullet} formed after the first PCET reaction is also accompanied by the proton release into the lumen ($PQH^{\bullet} + b_6^L(\text{ox}) \rightarrow PQ + b_6^L(\text{red}) + H_{\text{in}}^+$). The proton released from PQH^{\bullet} migrates to the lumen through the second putative proton-conducting channel (Tikhonov 2013, 2014). As noted above, it is likely that PQH^{\bullet} donates a proton to the neighboring acidic group ($-\text{COO}^-$) of Glu78 positioned in subunit IV between the quinone binding center Q_o and heme b_6^L (Fig. 10.7). From Glu78 the proton migrates to the lumen. The crystal structure of the Cyt *b₆f* complex from *M. laminosus* (Hasan et al. 2013c) suggests that the proton-accepting group of Glu3 located in subunit G may attract a proton from Glu78 and then release it to the aqueous bulk phase of the lumen.

Proton Entry Pathways At the PQ binding Q_i -center located on the “negative” (stromal) side of the Cyt *b₆f* complex, reduced PQ molecules undergo protonation through the proton-conductive pathways oriented towards the aqueous bulk phase of stroma. Refined crystal structure (2.70 Å) of the Cyt *b₆f* complex from *M. laminosus* (Hasan et al. 2013c) revealed a unique short pathway for proton transfer to the Q_i -site, which involves two residues of the Cyt *b₆* protein ($H_{\text{out}}^+(\text{aq}) \rightarrow \text{Asp20} \rightarrow \text{arg 207} \rightarrow Q_i$). The Asp20 side chain is located on the

surface of the Cyt *b₆f* complex; therefore, it has direct access to the aqueous phase. Both steps of the proton transfer within the Cyt *b₆* protein (Asp20 → Arg207 and Arg207 → Q_i) are mediated by hydrogen bonds. Arg207 has access to (PQ)_i as well as heme *c_i*. Another putative way of proton transfer may be mediated by the surface residues Lys24. In addition to these proton transfer pathways, the acidic side chains of Glu29 and Asp35 (subunit IV) may be involved in proton transfer from stroma to the PQ molecule, reduced at the Q_i-center (Hasan et al. 2013c).

10.3.2 Kinetics of Plastoquinol Oxidation

The elucidation of the mechanism of PQH₂ oxidation is a key to understanding the nature of the rate-limiting step in the intersystem ETC. Molecular machinery of quinol oxidation in the Cyt complexes of *bc* type have been scrutinized in a number of original works and related review articles (see Berry et al. 2000; Crofts 2004a, b; Crofts et al. 1999a, b, 2000, 2006, 2013; Mulkidjanian 2005; Xia et al. 2013). There are several events that have been considered to explain the nature of the rate-limiting step of quinol oxidation: (i) the formation of the quinol-ISP complex (Mulkidjanian 2005), (ii) deprotonation of the neutral quinol to the anionic form (PQH₂ → PQH⁻ + H_{in}⁺) and the formation of the “enzyme-substrate” complex (PQH⁻/ISP_{ox}) followed by PQH⁻ oxidation (Brandt and Okun 1997; Link 1997; Rich 2004), and (iii) constrained diffusion of the ISP mobile domain between the PQH₂ binding site Q_o and Cyt *f* (or Cyt *c₁*) (Izrailev et al. 1999; Crofts et al. 1999a, b; Darrouzet et al. 2001). Structural, kinetic and thermodynamic aspects of PQH₂ oxidation at the Q_o-site are considered below.

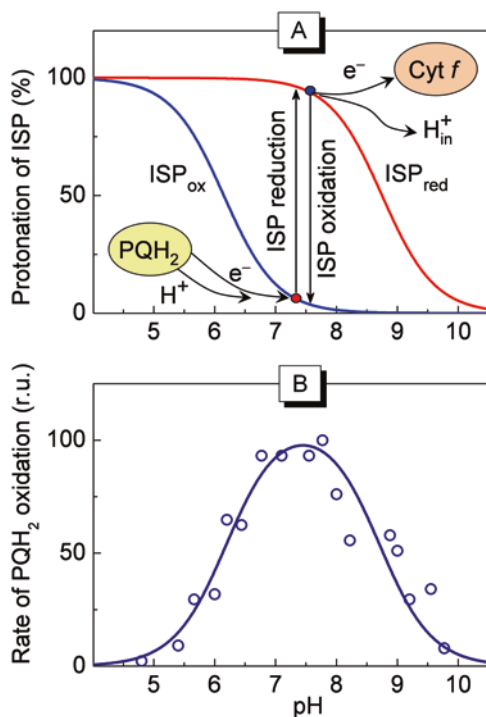
Structural and kinetic data suggest that the round-trip movements of the mobile domain of the ISP between the Q_o-site and heme *f* could determine only partly the turnover rate of the Cyt *b₆f* complex. A flexible “detail” of the ISP machinery (a “hinge”) provides restricted tethered diffusion of the extrinsic domain containing the redox [Fe₂S₂] cluster. However, the flip-flop motions of the [Fe₂S₂] cluster between the proximal and distal positions are rapid as compared to the rate of PQH₂ oxidation; therefore, they should not limit the overall rate of PQ turnover. According to (Yan and Cramer 2003; de Vitry et al. 2004), electron transfer from the ISP_{red} to heme *f* may occur more rapidly ($t_{1/2} \leq 2 - 4$ ms) than the overall rate of PQH₂ oxidation ($t_{1/2} \geq 4 - 20$ ms, Stiehl and Witt 1969; Haehnel 1984). This implies that the rate of PQH₂ oxidation should be determined predominantly by the processes associated with the formation of the substrate-enzyme complex PQH₂/ISP_{ox} and intrinsic reactions related to PQH₂ oxidation within the Cyt *b₆f* complex.

Analyzing experimental data on ubiquinol (UQH₂) oxidation in the *bc₁* complex in the purple photosynthetic bacterium *Rhodobacter sphaeroides*, Crofts and collaborators concluded that the activated step of UQH₂ oxidation was in a reaction step after the formation of the UQH₂/ISP_{ox} complex (Hong et al. 1999). The pH-dependence of the rate of UQH₂ oxidation reflected the p*K* of the oxidized ISP (ISP_{ox}) and requirement for the deprotonated form of ISP_{ox} in formation of the

UQH₂/ISP_{ox} complex. Conclusive argument in favor of the first electron transfer reaction as the rate-limiting step of quinol oxidation was based on experimental data in strains with mutations in the ISP that lowered its redox potential E_m . The overall rate of UQH₂ oxidation was determined by the driving force for the first electron transfer, $\Delta G_1^0 = -zF(E_{m(\text{ISP})} - E_{m(\text{QH}_2/\text{SQ})})$, but was almost independent of the driving force for the second electron transfer, $\Delta G_2^0 = -zF(E_{m(b_l)} - E_{m(\text{SQ}/\text{Q})})$ (Crofts 2004b; Crofts et al. 2013). This strongly suggests that the stage of electron transfer from the quinol molecule to ISP_{ox} is the rate-limiting step of bifurcated oxidation of quinol.

Electron transfer from quinol to the redox center of ISP_{ox} is tightly coupled to the concerted proton transfer to an appropriate proton-accepting group. As noted above, the N_ε atom of the histidine residue liganding to the Fe1 atom the [Fe₂S₂] cluster is the prime candidate for the role of the primary recipient of the proton donated by PQH₂. Figure 10.10a illustrates the scenario of protonation/deprotonation events associated with the reduction/oxidation of the ISP. The affinity of the ISP for protons depends on its redox state (Zu et al. 2003; Iwaki et al. 2005; Lin et al. 2006; Hsueh et al. 2010; Lhee et al. 2010). The deprotonated state of ISP_{ox} is likely an obligatory prerequisite for the first step of PQH₂ oxidation (Fig. 10.10a); therefore, the pK_{ox} value of the ISP_{ox} will determine the pH-dependence of the rate of this reaction. In photosynthetic systems of oxygenic type, the pK value of functional proton-accepting groups of ISP_{ox} is characterized by $pK_{\text{ox}} \approx 6 - 6.5$ (Finazzi 2002; Soriano et al. 2002). *Ex facte* the affinity of the ISP for a proton should increase with the acquisi-

Fig. 10.10 A diagram illustrating redox-dependent protonation/deprotonation of the ISP protein (A), and pH-dependence of PQH₂ oxidation by isolated cytochrome *b₆f* complex (B). Open circles shown in panel B are taken from Fig. 4 in (Hope et al. 1994); solid line represents the result of simulation according to Eq. (10.3) for parameters $pK_{\text{ox}} = 6.2$ and $pK_{\text{red}} = 8.7$ (see text for explanations) (Modified from Figure 9 in Tikhonov 2014)



tion of the negative charge by the redox cluster [Fe₂S₂]. That is why pK_{ox} increases to $pK_{\text{red}} \approx 8.3 - 8.9$ after the ISP reduction. This means that under the normal physiological conditions ($\text{pH}_{\text{in}} \leq \text{pH}_{\text{out}} \leq 8$) the ISP_{red} will keep tightly the proton accepted from PQH_2 . After oxidation of the reduced and protonated form of the ISP, its affinity to the proton decreases (Fig. 10.10a), and the proton will dissociate into the lumen via a proton-conducting channel ($\text{ISP}_{\text{red}}^{\cdot} \text{H}^+ + \text{Cyt } f_{\text{ox}} \rightarrow \text{ISP}_{\text{ox}} + \text{Cyt } f_{\text{red}} + \text{H}_{\text{in}}^+$).

Let us consider the pH-dependence of PQH_2 oxidation rate. At any given pH, the rate of PQH_2 oxidation will be controlled by two factors: (i) a probability of finding the oxidized ISP_{ox} in deprotonated state, $p(\text{ISP}_{\text{ox}})$, the value of which is determined by pK_{ox} , and (ii) a probability of finding reduced ISP in protonated state, $p(\text{ISP}_{\text{red}}^{\cdot} \text{H}^+)$, determined by the pK_{red} value. Therefore, the overall rate of PQH_2 oxidation, k_1 , will be proportional to the product $p(\text{ISP}_{\text{ox}}) \times p(\text{ISP}_{\text{red}}^{\cdot} \text{H}^+)$. Elementary calculations lead to the following term (Tikhonov 2014):

$$k_1 \propto 10^{pK_{\text{red}} - \text{pH}} \times \left(1 + 10^{pK_{\text{red}} - \text{pH}}\right)^{-1} \times \left(1 + 10^{pK_{\text{ox}} - \text{pH}}\right)^{-1}. \quad (10.3)$$

Equation (10.3) predicts the bell-shape pH-dependence of the rate constant k_1 , which reflects the pK_{ox} and pK_{red} values of the ISP. Figure 10.10b shows that formula (10.3) adequately describes experimental pH-dependence of the rate of PQH_2 oxidation by the Cyt *b₆f* complex if $pK_{\text{ox}} = 6.2$ and $pK_{\text{red}} = 8.7$ (Hope et al. 1994).

10.3.3 Energy Profiles of Electron Transport Reactions in the Q_o-Site

The energy profile of bifurcated oxidation of PQH_2 can shed additional light on the nature of this reaction. Thermodynamic aspects of PQH_2 oxidation can be illustrated by the comparison of the redox potential profiles for electron carriers of the high-potential ($\text{PQH}_2 \rightarrow \text{ISP} \rightarrow f \rightarrow \text{Pc} \rightarrow \text{P}_{700}$) and the low-potential ($\text{PQH}^{\cdot} \rightarrow b_6^{\text{L}} \rightarrow b_6^{\text{H}} \rightarrow c_i \rightarrow (\text{PQ})_i$) redox chains shown in Fig. 10.11. The overall change in Gibbs free energy upon the two-electron oxidation of PQH_2 is negative. As the result of complete turnover of PQH_2 in the Q-cycle, one electron extracted from PQH_2 reaches one of P_{700}^+ centers, and this is the energy-favorable (down-hill) processes. However, the fact of the matter is that the first step of PQH_2 oxidation (electron transfer $\text{PQH}_2 \rightarrow \text{ISP}_{\text{ox}}$ with the formation of PQH^{\cdot}) is the energy-uphill process, although the overall reaction of two-electron oxidation of PQH_2 is thermodynamically favorable process (Fig. 10.11). By analogy with the Cyt *bc₁* complex (for references, see Hong et al. 1999; Crofts et al. 2000; Crofts 2004a, b), it is safe to suggest that in the Cyt *b₆f* complex this stage of electron transfer proceeds through the energy barrier, which decelerates the overall reaction of PQH_2 oxidation. Plastosemiquinone PQH^{\cdot} formed in the result of the first electron transfer is a strong reductant capable of reducing the low-potential heme b_6^{L} . High reducing activity of PQH^{\cdot} is a general property of semiquinone species, because most of the redox

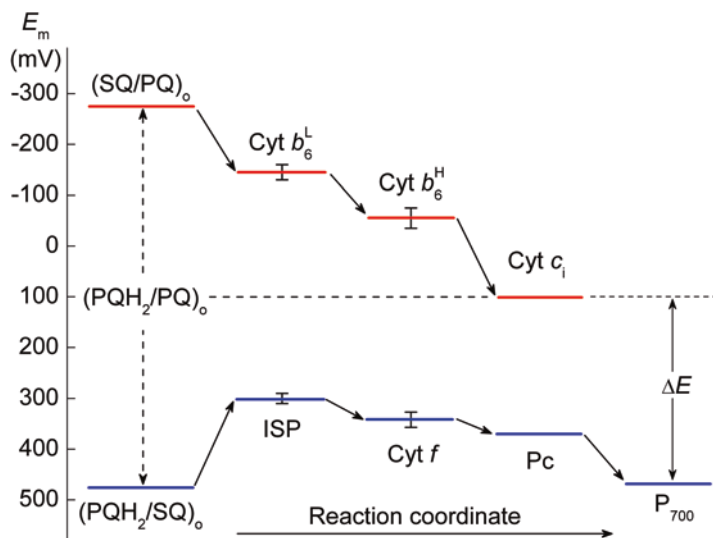


Fig. 10.11 A diagram of the midpoint redox-potentials of electron carriers of the high-potential (ISP, Cyt f , Pc, and P_{700}) and low-potential (hemes b_6^L , b_6^H , and c_1) branches of electron transport in the Cyt b_6f complex. The levels of the midpoint potentials shown here are the averaged values taken from the literature for *Chlamydomonas reinhardtii* (Alric et al. 2005; Hasan et al. 2013a; Nelson and Yocum 2006; Pierre et al. 1995; Zito et al. 1998)

couples SQ/Q are characterized by relatively low values of their redox potentials (Clark 1960). Further reactions of electron transfer along the low-potential and high-potential chains proceed spontaneously with the loss of free energy.

Let us compare the midpoint potentials of one-electron redox couples PQH_2/SQ and SQ/PQ ($E_{m(PQH_2/SQ)}$ and $E_{m(SQ/PQ)}$) involved in electron transport along the high- and low-potential chains (Fig. 10.11). For the redox couple PQH_2/PQ , the mid-point potential $E_{m(PQH_2/PQ)}$ can be measured directly, since PQH_2 and PQ are relatively stable species. However, direct determination of $E_{m(PQH_2/SQ)}$ and $E_{m(SQ/PQ)}$ is problematic, because semiquinones are extremely reactive species. These potentials may be evaluated indirectly (Mitchell 1976; Chobot et al. 2008) using the relationship (10.4):

$$E_{m(PQH_2/PQ)} = \frac{1}{2} \left(E_{m(PQH_2/SQ)} + E_{m(SQ/PQ)} \right). \quad (10.4)$$

According to Gill and Tuteja (2010) and Bleier and Dröse (2013), semiquinone species transiently formed in the Q_o -centers of the Cyt bc_1 and Cyt b_6f complexes are able to reduce molecular oxygen O_2 to superoxide radical, $O_2^{\cdot-}$. The standard redox potential relative to 10^5 Pa of O_2 is $E_{0(O_2^{\cdot-}/O_2)} = -330$ mV; the redox potential relative to 1 M O_2 equals to -160 mV (Wood 1988). This implies a rather low value for $E_{m(SQ/Q)}$. Assuming that $E_{m(Q^{\cdot-}/Q)} \approx -280$ mV is sufficient to provide generation of superoxide radicals in mitochondria, Snyder et al. (2000) inferred that $E_{m(UQH_2/SQ)} \sim 460$ mV. This potential falls in the broad range of $E_{m(UQH_2/SQ)}$ values

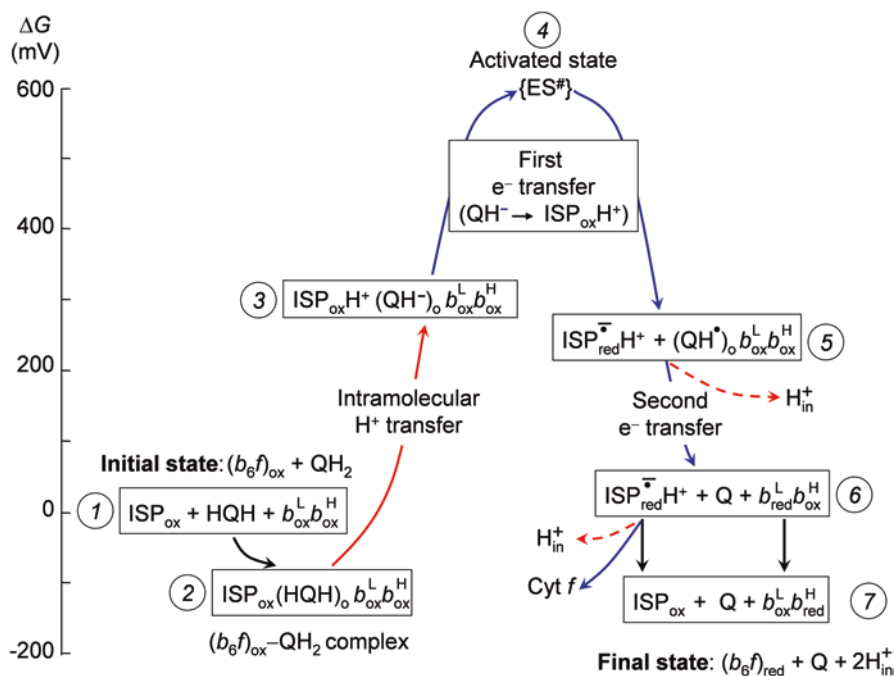


Fig. 10.12 Plausible energy profile of bifurcated two-electron reaction of quinol oxidation at the Q_o -site (Modified Figure 11 from Tikhonov 2014)

(from 310 to 776 mV) obtained from kinetic data for the Cyt bc_1 complex in *Rhodobacter sphaeroides* (Hong et al. 1999; Cape et al. 2007). Similar estimates were obtained from the measurements of SQ generation at the Q_o -site in the Cyt bc_1 complex (Cape et al. 2007). These estimates are in agreement with experimental evidence that in the Cyt complexes of the bc family the rate of quinol oxidation is largely determined by the first electron transfer reaction (see Crofts 2004a, b). Thus, taking into account the estimated values of $E_m(\text{PQH}_2/\text{SQ})$ and $E_m(\text{ISP})$ (Fig. 10.11), we can conclude that electron transfer from PQH_2 to the ISP_{ox} is the energy-uphill process that limits the overall rate of PQH_2 oxidation (see also Malnož et al. 2011). The increase in free energy upon the first electron transfer ($\text{PQH}_2 \rightarrow \text{ISP}_{\text{ox}}$) is compensated by the free energy decrease in the energy-favorable reactions $\text{SQ} \rightarrow b_6^{\text{L}} \xrightarrow{e^-} b_6^{\text{H}}$.

Figure 10.12 depicts the sequence of events associated with the reaction of PQH_2 oxidation according to the “proton-first-then-electron” (PT/ET) transfer mechanism favoured by Crofts et al. (2013). After the formation of the PQH_2 - ISP_{ox} complex (the downhill transition $1 \rightarrow 2$), the proton transfer from PQH_2 to the ISP_{ox} occurs (the uphill transition $2 \rightarrow 3$). This step is accompanied by the free energy rise $DG_{\text{proton}} = 2.303 \times RT \times (\text{p}K_{\text{PQH}_2} - \text{p}K_{\text{ISP}_{\text{ox}}}) > 0$ (the so-called “Brønsted barrier”). The transfer of a proton towards the ISP moiety promotes the electron transfer, resulting in the production of $\text{ISP}_{\text{red}}^{\text{H}^+}$ and PQH^{\bullet} (the transition $3 \rightarrow 4 \rightarrow 5$ over the activation barrier 4). $\text{ISP}_{\text{red}}^{\text{H}^+}$ dissociates from the Q_o -center and moves towards

heme *f* (state 5). Then, after the second PCET reaction, oxidized quinone dissociates from the Q_o -center (the downhill transition $5 \rightarrow 6$). Further electron transfer (the downhill transition $6 \rightarrow 7$) will stabilize charge separation after the completion of the PQH₂ oxidation cycle at the Q_o -site.

Quantum chemical calculations for a model system consisting of TMQH₂ (trimethylbenzoquinol, the “bobtail” analog of PQH₂), the [Fe₂S₂] cluster, and surrounding them amino acid residues of the Cyt *b₆f* complex (Fig. 10.13a), support the notion that the PCET from PQH₂ to ISP_{ox} is the “uphill” process, which hampers the overall rate of PQH₂ oxidation (Frolov and Tikhonov 2009). According to density functional theory (DFT) computations, the transfer of a hydrogen atom from the quinol molecule to the nearest nitrogen atom of His155 is the endoergonic process ($\Delta E \approx 10$ kcal/mol) with a rather high energy barrier (Fig. 10.13b). The rate constant for this process was calculated using the Moser–Dutton ruler for evaluation of the rate of electron tunneling between redox centers (Page et al. 1999) expanded by Crofts (2004b) for PCET reactions. The rate constant of TMQH₂ oxidation in the model system was evaluated as $k_{\text{PCET}} \sim 40 - 170 \text{ s}^{-1}$ (Frolov and Tikhonov 2009). These estimates correspond to the half-times of PQH₂ oxidation $t_{1/2} = \ln 2/k_{\text{PCET}} \sim 4 - 17 \text{ ms}$. These values are in a reasonably good agreement with experimental data for electron transfer from PQH₂ to P₇₀₀⁺ (Sect. 10.2.5).

What type of the mechanism for electron transfer in the Q_o -centers, “sequential” or “concerted”, is realized in the Cyt *b₆f* and *bc₁* complexes? This question still remains a challenge to molecular bioenergetics. “Sequential” mechanism (PQH₂ $\xrightarrow{-e^-}$ SQ $\xrightarrow{-e^-}$ PQ) implies that the first and the second electron transfer reactions occur separately, with a certain time-delay between the steps. In this case, SQ radicals appear transiently as the intermediate species (Cape et al. 2006). A genuine “concerted” mechanism implies that the long-lived SQ species will not form if the bifurcated oxidation of PQH₂ proceeds in a single step as a time-concerted transfer of two electrons (Osyczka et al. 2004, 2005). In the latter case, both steps are realized simultaneously (within picoseconds-microseconds), with no SQ intermediate available to participate in side reactions. The truly concerted mechanism could be realized when both the redox partners, the [Fe₂S₂] cluster and heme *b₆^L*, are oxidized. Simultaneous reduction of ISP and Cyt *b_L* with $t_{1/2} \sim 250$ microsecond was observed during ubiquinol oxidation in the bovine Cyt *bc₁* complex (Zhu et al. 2007). Concerted oxidation of PQH₂ precludes the accumulation of SQ, thereby avoiding the formation of harmful superoxide radicals (SQ \rightarrow O₂⁻) (Cape et al. 2006).

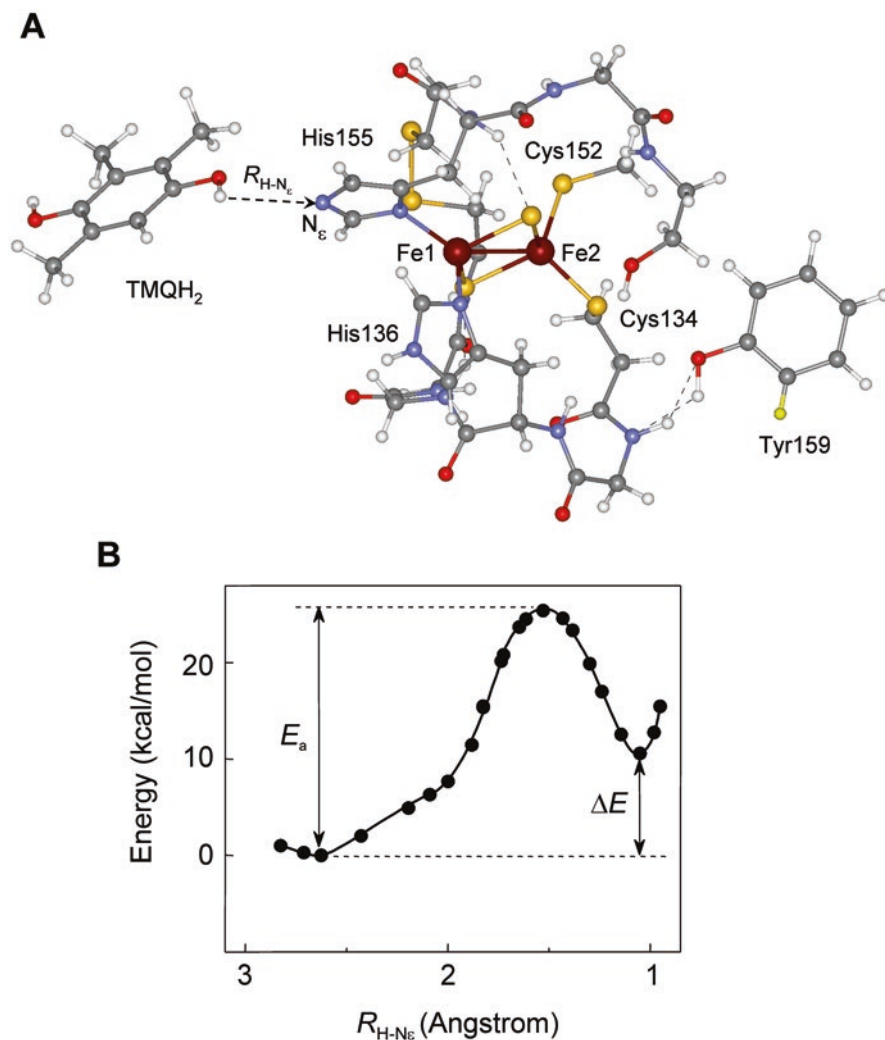


Fig. 10.13 Panel A – Quantum chemical part of the model system, which includes trimethylbenzoquinol (TMQH₂, the analogue of PQH₂), the [Fe₂S₂] cluster, and surrounding them amino acid residues of the Cyt *b_f* complex, Cys134-Thr135-His136-Leu137-Gly138-Cys139, Cys152, Cys154-His155-Gly156-Ser157, Tyr159 (Frolov and Tikhonov 2009). TMQH₂ was placed at the position of quinone inhibitor TDS in the crystal structure of the Cyt *b_f* complex from *Chlamydomonas reinhardtii* (PDB entry 1Q90, Stroebel et al. 2003)

Panel B – The plot of the model system energy *versus* the reaction coordinate $R_{H-N_{\epsilon}}$, which simulates changes in the potential energy of the model system upon the displacement of the H atom from TMQH₂ to the N_ε atom of His155 (after Frolov and Tikhonov 2009)

10.4 Regulation of the Intersystem Electron Transport

10.4.1 *pH-Dependent Control of the Intersystem Electron Transport*

Apart from the role of the molecular device for electron transport and proton pumping, the Cyt *b₆f* complex participates in feedback regulation of electron transport. The light-induced acidification of the thylakoid lumen is the key factor of down-regulation of the intersystem electron transport (Rumberg and Siggel 1969; Tikhonov et al. 1981, 1984; Harbinson and Hedley 1989; Foyer et al. 2012; Järvi et al. 2013; Tikhonov 2013). Down-regulation of the intersystem electron transport is associated with two basic effects caused by the light-induced decrease in the intrathylakoid pH_{in} : (i) the retardation of PQH_2 oxidation, and (ii) the attenuation of PSII activity. The first mechanism of electron transport control is realized in the stage of PQH_2 oxidation at the Q_o -site of the Cyt *b₆f* complex (for review, see Tikhonov 2013, 2014, 2015). Acidification of the lumen impedes the oxidation of PQH_2 due to the back “pressure” from the protons accumulating inside the thylakoids on the functional proton-accepting groups, thereby decreasing the rate of PQH_2 oxidation (Figs. 10.5b and 10.10b). The influence of pH_{in} on the rate of PQH_2 oxidation is likely to reflect the effect of pH_{in} on the formation of hydrogen bonds between PQH_2 and the nearby proton-accepting groups in the Q_o -center (the N_ϵ atom of His155/His129 and the carboxyl group of Glu78). Note that electron transfer from Cyt *f* to Pc is independent of pH_{in} (Finazzi 2002). Acidification of the lumen also acts as a signal for enhancement of excess energy dissipation in the light-harvesting antenna of PSII, i.e., non-photochemical quenching (NPQ) of Chl *a* excitation (Eberhard et al. 2008; Horton 2012; Ruban 2012). Both mechanisms, the slowing down of PQ turnover and generation of NPQ, cause deceleration of electron flow from PSII to PSI at excess of irradiation, protecting PSA against solar stress (for review, see Li et al. 2009, Demmig-Adams et al. 2012, Horton 2012, Rochaix 2014, Jallet et al. 2016).

10.4.2 *Redox-Dependent Regulation of Electron Transport and State Transitions*

Other regulatory mechanisms are associated with the light-induced activation of metabolic processes and redistribution of electrons fluxes between alternative electron transport pathways, which are controlled by the redox state of the chloroplast ETC. The light-induced activation of the CBC reactions is a striking example of pH- and redox-dependent regulation of metabolic processes in photosynthetic systems. The CBC is inactive in dark-adapted chloroplasts. The light-induced alkalization of stroma and redox-dependent activation of the CBC enzymes speed up the outflow of electrons from PSI to the CBC (Buchanan 1980; Edwards and Walker

1983; Andersson 2008; Michelet et al. 2013; Balsera et al. 2016). In addition to acceleration of LEF (PSII \rightarrow PSI \rightarrow CBC) due to activation of the CBC reactions, there are redox-dependent mechanisms of redistribution of electron fluxes between the LEF and CEF1 pathways. The partitioning of electron fluxes on the donor side of PSI is controlled by competition between the LEF and CEF1 pathways for reducing equivalents (Joliot and Joliot 2005; Breyton et al. 2006; Johnson 2011). Relatively slow consumption of NADPH in the CBC, which is peculiar to dark-adapted chloroplasts, would divert electrons from LEF to CEF1, thereby supporting generation of ΔpH and ATP synthesis (Kramer et al. 2004). In the meantime, with the light-induced activation of the CBC reactions, the contribution of CEF1 will decrease in favor of LEF.

The mechanism of electron transport control associated with the redistribution of light energy between the light-harvesting complexes of PSI and PSII is triggered by the “check-point device” operating at the level of the Cyt *b₆f* complex. This regulatory mechanism relates to the so-called “state transitions” phenomenon. It is well established fact that the redox state of the PQ pool serves as a signal about the “traffic jam” on the pathway between PSII and PSI (see Bennett 1977; Allen 1992; Haldrup et al. 2001; Lemeille and Rochaix 2010; Rochaix 2014; Puthiyaveetil et al. 2016). The over-reduction of the PQ pool triggers a protein kinase that catalyses phosphorylation of the loosely bound light-harvesting complexes of PSII. This process is induced by PQH₂ binding to the Q_o-site of the Cyt *b₆f* complex (Vener et al. 1997; Zito et al. 1999). In plants, there are three forms of LHCII trimers, which differ with respect to their association with PSII: “strong”, “moderate”, and “loose” binding to PSII (Galka et al. 2012; Puthiyaveetil et al. 2016). The loosely bound form of phosphorylated LHCII dissociates from the PSII-LHCII supercomplex and migrates to PSI, thereby increasing the light harvesting capacity of PSI (see cartoon in Fig. 10.14). Such a structural remodelling of PSA, termed “State 1 \rightarrow State 2” transition, enhances PSI activity at expense of PSII, promoting the reoxidation of the PQH₂ pool. Redistribution of energy in favour of PSI is a reversible process: after a decrease in the concentration of PQH₂, LHCII becomes dephosphorylated due to chloroplast phosphatases. Dephosphorylation of LHCII allows its return to the grana domains enriched with PSII (“State 2 \rightarrow State 1” transition), increasing the light absorption in PSII. Remodelling of PSA associated with state transitions provides short-term responses (in the minute range) of photosynthetic organisms to variations of light intensity. Thus, reversible transitions “State 1 \leftrightarrow State 2” provide the optimal balance of absorbed light energy between PSI and PSII upon fluctuations of the environment light (Tikkanen and Aro 2012, Tikkanen et al. 2012).

A molecular device, which receives the signal from the PQH₂ pool and triggers state transitions, is inherent to the Cyt *b₆f* complex. Activation of the LHCII kinase is initiated by PQH₂ binding to the Q_o-site. A strong correlation between the PQH₂ occupancy at the Q_o-center and the LHCII kinase activity of chloroplasts has been found in (Vener et al. 1997, Zito et al. 1999). In *C. reinhardtii*, activation of the LHCII kinase is mediated through the protein kinase Stt7, which becomes phosphorylated in State 2 conditions. Protein kinase Stt7 acts in catalytic amounts (Stt7/LHCII \sim 1/200) (Lemeille et al. 2009). Stt7 has an ortholog STN7 in *Arabidopsis*

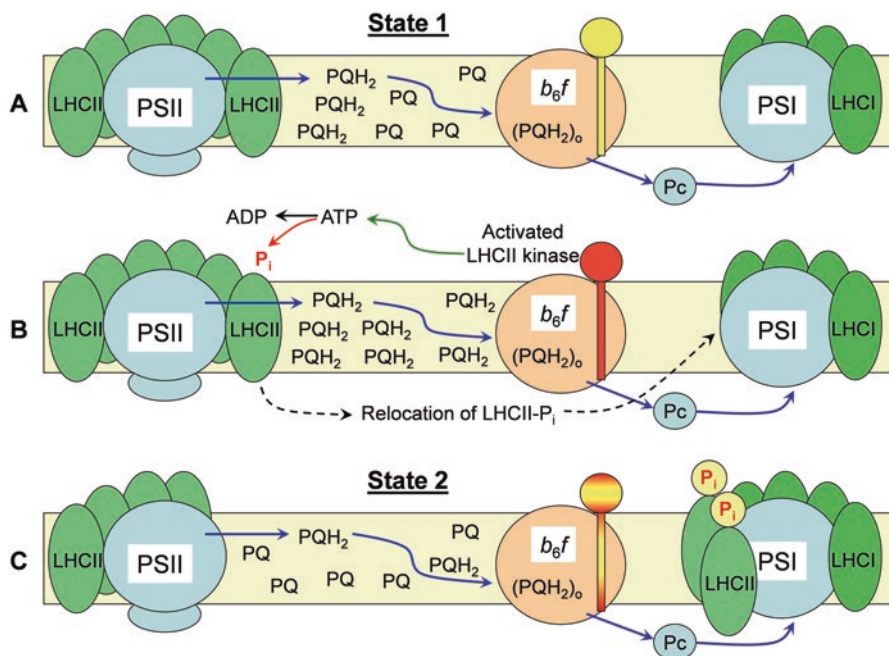


Fig. 10.14 A schematic representation of state transitions triggered by the PQH₂ binding to the Cyt *b₆f* complex (see explanations in text) (Modified Figure 15 from Tikhonov 2014)

and other land plants (Bellafore et al. 2005). The knock out of STN7 inhibits phosphorylation of LHCII and state transitions. A putative mechanism of kinase activation due to PQH₂-induced conformational changes in the Cyt *b₆f* complex has been suggested in (Hasan et al. 2013a). However, a complete chain of events leading to state transitions is still unclear. The Stt7/STN7 kinase is the redox-regulated enzyme, which contains the catalytic and regulatory domains (Bellafore et al. 2005; Lemeille et al. 2009). The catalytic domain is facing the stroma, the regulatory domain is exposed to the thylakoid lumen. These domains are separated by a transmembrane helix with two Cys residues essential for the enzyme activity. The redox state of Cys residues may be regulated by Fd and thioredoxin through the membrane-bound thiol oxidoreductases (Lennartz et al. 2001; Motohashi and Hisabori 2006; Dietz and Pfannschmidt 2011). The over-reduced electron acceptors on the acceptor side of PSI will cause the reduction of Cys residues, thereby promoting dephosphorylation of the kinase and eventually inducing the “State 2 → State 1” transition, upon which PSI activity will lessen.

10.5 Concluding Remarks

Summing up a brief overview of structural and functional properties of the Cyt *b₆f* complex, one can conclude that the overall rate of quinol oxidation is determined by PQH₂ turnover at the Q_o-site. The rates of PQ reduction to PQH₂ in PSII and its diffusion to the Cyt *b₆f* complex do not limit the overall rate of electron transfer between PSII and PSI. The rate-limiting step in the intersystem electron transport is associated with PQH₂ oxidation at the Q_o-site in the Cyt *b₆f* complex. It is the first step of the bifurcated reaction of PQH₂ oxidation (electron transfer from PQH₂ to ISP_{ox}) that restricts the rate of PQH₂ oxidation. The rate of this process is controlled by the intrathylakoid pH, values of which determine the protonation/deprotonation events in the Q_o-center of the Cyt *b₆f* complex. The feedback control of PQH₂ oxidation is governed by the intrathylakoid pH_{in}. The acidification of the lumen causes deceleration of PQH₂ oxidation, thus impeding the intersystem electron transport. The Cyt *b₆f* complex stands at the crossroad of alternative pathways of electron transport, providing flexibility and adaptability of the photosynthetic apparatus by means of two regulatory mechanisms: (i) redistribution of electron fluxes between alternative pathways (LEF and CEF1), and (ii) “state transitions” associated with the redistribution of solar energy between PSI and PSII.

Acknowledgments This work was supported in part by the Russian Foundation for Basic Research (RFBR Project 15-04-03790a).

References

- Albertsson PÅ (2001) A quantitative model of the domain structure of the photosynthetic membrane. *Trends Plant Sci* 6:349–354
- Allen JF (1992) Protein phosphorylation in regulation of photosynthesis. *Biochim Biophys Acta* 1098:275–335
- Allen JF (2003) Cyclic, pseudocyclic and noncyclic photophosphorylation: new links in the chain. *Trends Plant Sci* 8:15–19
- Alric J, Pierre Y, Picot D et al (2005) Spectral and redox characterization of the heme *c₁* of the cytochrome *b₆f* complex. *Proc Natl Acad Sci U S A* 102:15860–15865
- Anderson JM (1982) Distribution of the cytochromes of spinach chloroplasts between the appressed membranes of grana stacks and stroma-exposed thylakoid regions. *FEBS Lett* 138:62–66
- Anderson JM, Chow WS, Goodchild DJ (1988) Thylakoid membrane organisation in sun/shade acclimation. *Funct Plant Biol* 15:11–26
- Andersson I (2008) Catalysis and regulation in Rubisco. *J Exp Bot* 59:1555–1568
- Balsera M, Schürmann P, Buchanan BB (2016) Redox regulation in chloroplasts. In: Kirchhoff H (ed) *Chloroplasts. Current research and future trends*. Caister Academic Press, Norfolk, pp 187–207
- Bellaïf S, Barneche F, Peltier G et al (2005) State transitions and light adaptation require chloroplast thylakoid protein kinase STN7. *Nature* 433:892–895
- Bendall DS, Manasse RS (1995) Cyclic photophosphorylation and electron transport. *Biochim Biophys Acta* 1229:23–38
- Bennett J (1977) Phosphorylation of chloroplast membrane polypeptides. *Nature* 269:344–346

- Benz JP, Lintala M, Soll J et al (2010) A new concept for ferredoxin-NADP(H) oxidoreductase binding to plant thylakoids. *Trends Plant Sci* 15:608–613
- Berry EA, Guergova-Kuras M, Huang L et al (2000) Structure and function of cytochrome *bc* complexes. *Annu Rev Biochem* 69:1005–1075
- Blankenship RE (2002) Molecular mechanisms of photosynthesis. Blackwell Science, Oxford
- Bleier L, Dröse S (2013) Superoxide generation by complex III: from mechanistic rationales to functional consequences. *Biochim Biophys Acta* 1827:1320–1231
- Brandt U (1996) Bifurcated ubihydroquinone oxidation in the cytochrome *bc₁* complex by protonated charge transfer. *FEBS Lett* 387:1–6
- Brandt U, Okun JG (1997) Role of deprotonation events in ubihydroquinone: cytochrome *c* oxidoreductase from bovine heart and yeast mitochondria. *Biochemistry* 36:11234–11240
- Brettel K (1997) Electron transfer and arrangement of the redox cofactors in photosystem I. *Biochim Biophys Acta* 1318:322–373
- Breyton C (2000) Conformational changes in the cytochrome *b₆f* complex induced by inhibitor binding. *J Biol Chem* 275:13195–13201
- Breyton C, Nandha B, Johnson G et al (2006) Redox modulation of cyclic electron flow around photosystem I in C3 plants. *Biochemistry* 45:13465–13475
- Buchanan BB (1980) Role of light in the regulation of chloroplast enzymes. *Annu Rev Plant Physiol* 31:341–374
- Burrows PA, Sazanov LA, Svab Z et al (1998) Identification of a functional respiratory complex in chloroplasts through analysis of tobacco mutants containing disrupted plastid *ndh* genes. *EMBO J* 17:868–876
- Cape JL, Bowman MK, Kramer DM (2006) Understanding the cytochrome *bc* complexes by what they don't do. The Q-cycle at 30. *Trends Plant Sci* 11:46–55
- Cape JL, Bowman MK, Kramer DM (2007) A semiquinone intermediate generated at the Q_o site of the cytochrome *bc₁* complex: importance for the Q-cycle and superoxide production. *Proc Natl Acad Sci U S A* 104:7887–7892
- Cardona T, Sedoud A, Cox N et al (2012) Charge separation in Photosystem II: a comparative and evolutionary overview. *Biochim Biophys Acta* 1817:26–43
- Chobot SE, Zhang H, Moser CC et al (2008) Breaking the Q-cycle: finding new ways to study Q_o through thermodynamic manipulations. *J Bioenerg Biomembr* 40:501–507
- Chovancová E, Pavelka A, Beneš P et al (2012) CAVER 3.0: a tool for the analysis of transport pathways in dynamic protein structures. *PLoS Comput Biol* 8:e1002708
- Clark WM (1960) Oxidation-reduction potentials of organic systems. Williams and Wilkins, Baltimore
- Cramer WA, Zhang H, Yan J et al (2006) Transmembrane traffic in the cytochrome *b₆f* complex. *Annu Rev Biochem* 75:769–790
- Cramer WA, Hasan SS, Yamashita E (2011) The Q cycle of cytochrome *bc* complexes: A structure perspective. *Biochim Biophys Acta* 1807:788–802
- Crofts AR (2004a) The cytochrome *bc₁* complex: function in the context of structure. *Annu Rev Physiol* 66:689–733
- Crofts AR (2004b) Proton-coupled electron transfer at the Q_o-site of the *bc₁* complex controls the rate of ubihydroquinone oxidation. *Biochim Biophys Acta* 1655:77–92
- Crofts AR, Guergova-Kuras M, Huang L-S et al (1999a) Mechanism of ubiquinol oxidation by the *bc₁* complex: role of the iron sulfur protein and its mobility. *Biochemistry* 38:15791–15806
- Crofts AR, Hong S, Zhang Z et al (1999b) Physicochemical aspects of the movement of the Rieske iron sulfur protein during quinol oxidation by the *bc₁* complex from mitochondria and photosynthetic bacteria. *Biochemistry* 38:15827–15839
- Crofts AR, Guergova-Kuras M, Kuras R et al (2000) Proton-coupled electron transfer at the Q_o-site: what type of mechanism can account for the high activation barrier? *Biochim Biophys Acta* 1459:456–466
- Crofts AR, Lhee S, Crofts SB et al (2006) Proton pumping in the *bc₁* complex: a new gating mechanism that prevents short circuits. *Biochim Biophys Acta* 1757:1019–1034

- Crofts AR, Hong S, Wilson C et al (2013) The mechanism of ubihydroquinone oxidation at the Q_o -site of the cytochrome bc_1 complex. *Biochim Biophys Acta* 1827:1362–1377
- Cruz JA, Avenson TJ, Kanazawa A et al (2007) Plasticity in light reactions of photosynthesis for energy production and photoprotection. *J Exp Bot* 56:395–406
- DalCorso G, Pesaresi P, Masiero S et al (2008) A complex containing PGRL1 and PGR5 is involved in the switch between linear and cyclic electron flow in *Arabidopsis*. *Cell* 132:273–285
- Darrouzet E, Moser CC, Dutton PL et al (2001) Large scale domain movement in cytochrome bc_1 : a new device for electron transfer in proteins. *Trends Biochem Sci* 26:445–451
- de Vitry C, Ouyang Y, Finazzi G et al (2004) The chloroplast Rieske iron-sulfur protein: at the crossroad of electron transport and signal transduction. *J Biol Chem* 279:44621–44627
- Dekker JP, Boekema EJ (2005) Supermolecular organization of the thylakoid membrane proteins in green plants. *Biochim Biophys Acta* 1706:12–39
- Demmig-Adams B, Cohu CM, Muller O et al (2012) Modulation of photosynthetic energy conversion efficiency in nature: from seconds to seasons. *Photosynth Res* 113:75–88
- Dietz K-J, Pfannschmidt T (2011) Novel regulators in photosynthetic redox control of plant metabolism and gene expression. *Plant Physiol* 155:1477–1485
- Eberhard S, Finazzi G, Wollman FA (2008) The dynamics of photosynthesis. *Annu Rev Genet* 42:463–515
- Edwards GE, Walker DA (1983) C_3 , C_4 : mechanisms, and cellular and environmental regulation of photosynthesis. Blackwell, Oxford
- Endo T, Shikanai T, Sato F et al (1998) NAD(P)H dehydrogenase-dependent, antimycin A-sensitive electron donation to plastoquinone in tobacco chloroplasts. *Plant Cell Physiol* 39:1226–1231
- Esser L, Gong X, Yang S et al (2006) Surface-modulated motion switch: capture and release of iron-sulfur protein in the cytochrome bc_1 complex. *Proc Natl Acad Sci U S A* 103:13045–13050
- Finazzi G (2002) Redox-coupled proton pumping activity in cytochrome b_6/f , as evidenced by the pH dependence of electron transfer in whole cells of *Chlamydomonas reinhardtii*. *Biochemistry* 41:7475–7482
- Foyer CH, Neukermans J, Queval G et al (2012) Photosynthetic control of electron transport and the regulation of gene expression. *J Exp Bot* 63:1637–1661
- Frolov AE, Tikhonov AN (2009) The oxidation of plastoquinol by a cytochrome b_6/f complex: a density functional theory study. *Russian J Phys Chem A* 83:506–508
- Fromme P, Jordan P, Krauss N (2001) Structure of photosystem I. *Biochim Biophys Acta* 1507:5–31
- Galka P, Santabarbara S, Khuong TTH et al (2012) Functional analyses of the plant photosystem I-light-harvesting complex II supercomplex reveal that light-harvesting complex II loosely bound to Photosystem II is a very efficient antenna for Photosystem I in state II. *Plant Cell* 24:2963–2978
- Gill SS, Tuteja N (2010) Reactive oxygen species and antioxidant machinery in abiotic stress tolerance in crop plants. *Plant Physiol Biochem* 48:909–930
- Haehnel W (1973) Electron transport between plastoquinone and chlorophyll a_1 . *Biochim Biophys Acta* 305:618–631
- Haehnel W (1976a) The reduction kinetics of chlorophyll a_1 as an indicator for proton uptake between the light reactions in chloroplasts. *Biochim Biophys Acta* 440:506–521
- Haehnel W (1976b) The ratio of the two light reactions and their coupling in chloroplasts. *Biochim Biophys Acta* 423:499–509
- Haehnel W (1982) On the functional organization of electron transport from plastoquinone to photosystem I. *Biochim Biophys Acta* 682:245–247
- Haehnel W (1984) Photosynthetic electron transport in higher plants. *Annu Rev Plant Physiol* 35:659–693
- Haldrup A, Jensen PE, Lunde C, Scheller HV (2001) Balance of power: a view of the mechanism of photosynthetic state transitions. *Trends Plant Sci* 6:301–305
- Harbinson J, Hedley CL (1989) The kinetics of P-700⁺ reduction in leaves: a novel *in situ* probe of thylakoid functioning. *Plant Cell and Environ* 12:357–369

- Hasan SS, Yamashita E, Cramer WA (2013a) Transmembrane signaling and assembly of the cytochrome *b₆f*-lipidic charge transfer complex. *Biochim Biophys Acta* 1827:1295–1308
- Hasan SS, Stoffleth JT, Yamashita E et al (2013b) Lipid-induced conformational changes within the cytochrome *b₆f* complex in oxygenic photosynthesis. *Biochemistry* 52:2649–2654
- Hasan SS, Yamashita E, Baniulis D et al (2013c) Quinone-dependent proton transfer pathways in the photosynthetic cytochrome *b₆f* complex. *Proc Natl Acad Sci* 110:4297–4302
- Heimann S, Ponamarev MV, Cramer WA (2000) Movement of the Rieske iron-sulfur protein in the p-side bulk aqueous phase: effect of luminal viscosity on redox reactions of the cytochrome *b₆f* complex. *Biochemistry* 39:2692–2699
- Hertle AP, Blunder T, Wunder T et al (2013) PGRL1 is the elusive ferredoxin-plastoquinone reductase in photosynthetic cyclic electron flow. *Mol Cell* 49:511–523
- Hong SJ, Ugulava N, Guergova-Kuras M et al (1999) The energy landscape for ubihydroquinone oxidation at the Q_o-site of the *bc₁* complex in *Rhodobacter sphaeroides*. *J Biol Chem* 274:33931–33944
- Hope AB (2000) Electron transfers amongst cytochrome *f*, plastocyanin and photosystem I: kinetics and mechanisms. *Biochim Biophys Acta* 1456:5–26
- Hope AB, Valent P, Matthews DB (1994) Effects of pH on the kinetics of redox reactions in and around the cytochrome *bf* complex in an isolated system. *Photosynth Res* 42:111–120
- Horton P (2012) Optimization of light harvesting and photoprotection: molecular mechanisms and physiological consequences. *Phil Trans R Soc B* 367:3455–3465
- Hsueh K-L, Westler WM, Markley JL (2010) NMR investigations of the Rieske protein from *Thermus thermophilus* support a coupled proton and electron transfer mechanism. *J Am Chem Soc* 132:7908–7918
- Iwai M, Takizawa K, Tokutsu R et al (2010) Isolation of the elusive supercomplex that drives cyclic electron flow in photosynthesis. *Nature* 464:1210–1213
- Iwaki M, Yakovlev G, Hirst J et al (2005) Direct observation of redox-linked histidine protonation changes in the iron–sulfur protein of the cytochrome *bc₁* complex by ATR-FTIR spectroscopy. *Biochemistry* 44:4230–4237
- Iwata S, Lee JW, Okada K et al (1998) Complete structure of the 11-subunit bovine mitochondrial cytochrome *bc₁* complex. *Science* 281:64–71
- Izrailev S, Crofts AR, Berry EA et al (1999) Steered molecular dynamics simulation of the Rieske subunit motion in the cytochrome *bc₁* complex. *Biophys J* 77:1753–1768
- Jallet D, Cantrell M, Peers G (2016) New players for photoprotection and light acclimation. In: Kirchhoff H (ed) *Chloroplasts. Current research and future trends*. Caister Academic Press, Norfolk, pp 133–159
- Järvi S, Gollan PJ, Aro E-M (2013) Understanding the roles of the thylakoid lumen in photosynthetic regulation. *Front Plant Sci*. <https://doi.org/10.3389/fpls.2013.00434>
- Joët T, Cournac L, Horvath EM et al (2001) Increased sensitivity of photosynthesis to antimycin A induced by inactivation of the chloroplast *ndhB* gene. Evidence for a participation of the NADH-dehydrogenase complex to cyclic electron flow around photosystem I. *Plant Physiol* 125:1919–1929
- Johnson GN (2011) Physiology of PSI cyclic electron transport in higher plants. *Biochim Biophys Acta* 1807:906–911
- Joliot P, Joliot A (2005) Quantification of cyclic and linear flows in plants. *Proc Natl Acad Sci U S A* 102:4913–4918
- Joliot P, Joliot A (2006) Cyclic electron flow in C3 plants. *Biochim Biophys Acta* 1757:362–368
- Jordan P, Fromme P, Witt HT et al (2001) Three-dimensional structure of photosystem I at 2.5 Å resolution. *Nature* 411:909–917
- Junge W, Nelson N (2015) ATP synthase. *Annu Rev Biochem* 83:631–657
- Kim H, Xia D, Yu CA et al (1998) Inhibitor binding changes domain mobility in the iron–sulfur protein of the mitochondrial *bc₁* complex from bovine heart. *Proc Natl Acad Sci U S A* 95:8026–8033

- Kirchhoff H (2008) Significance of protein crowding, order and mobility for photosynthetic membrane functions. *Biochem Soc Trans* 36:967–970
- Kirchhoff H (2013) Architectural switches in plant thylakoid membranes. *Photosynth Res* 116:481–487
- Kirchhoff H (2014) Diffusion of molecules and macromolecules in thylakoid membranes. *Biochim Biophys Acta* 1837:495–502
- Kono M, Terashima I (2014) Long-term and short-term responses of the photosynthetic electron transport to fluctuating light. *J Photochem Photobiol B* 137:89–99
- Kono M, Noguchi K, Terashima I (2014) Roles of cyclic electron flow around PSI (CEF-PSI) and O₂-dependent alternative pathways in regulation of the photosynthetic electron flow in short-term fluctuating light in *Arabidopsis thaliana*. *Plant Cell Physiol* 55:990–1004
- Kramer DM, Sacksteder CA, Cruz JA (1999) How acidic is the lumen? *Photosynth Res* 60:151–163
- Kramer DM, Avenson TJ, Edwards GE (2004) Dynamic flexibility in the light reactions of photosynthesis governed by both electron and proton transfer reactions. *Trends Plant Sci* 9:349–357
- Kubicki A, Funk E, Westhoff P et al (1996) Differential expression of plastome-encoded *ndh* genes in mesophyll and bundle-sheath chloroplasts of the C₄ plant *Sorghum bicolor* indicates that the complex I-homologous NAD(P)H-plastoquinone oxidoreductase is involved in cyclic electron transport. *Planta* 199:276–281
- Kubota K, Sakurai I, Katayama K et al (2009) Purification and characterization of photosystem I complex from *Synechocystis* sp. PCC 6803 by expressing histidine-tagged subunits. *Biochim Biophys Acta* 1797:98–105
- Kurisu G, Zhang H, Smith JL et al (2003) Structure of the cytochrome *b₆f* complex of oxygenic photosynthesis: tuning the cavity. *Science* 302:1009–1014
- Laisk A, Eichelmann H, Oja V et al (2005) Control of cytochrome *b₆f* at low and high light intensity and cyclic electron transport in leaves. *Biochim Biophys Acta* 1708:79–90
- Lavergne J, Joliot P (1991) Restricted diffusion in photosynthetic membranes. *Trends Biochem Sci* 16:129–134
- Lemeille S, Rochaix J-D (2010) State transitions at the crossroad of thylakoid signaling pathways. *Photosynth Res* 106:33–46
- Lemeille S, Willig A, Depège-Fargeix N et al (2009) Analysis of the chloroplasts protein kinase *Stt7* during state transition. *PLoS Biol* 7:e1000045, 664–673
- Lennartz K, Plucken H, Seidler A et al (2001) *HCF164* encodes a thioredoxin-like protein involved in the biogenesis of the cytochrome *b₆f* complex in *Arabidopsis*. *Plant Cell* 13:2539–2551
- Lhee S, Kolling DRJ, Nair SK et al (2010) Modifications of protein environment of the [2Fe-2S] cluster of the *bc₁* complex: effects on biophysical properties of the Rieske iron-sulfur protein and on the kinetics of the complex. *J Biol Chem* 285:9233–9248
- Li Z, Wakao S, Fischer BB et al (2009) Sensing and responding to excess light. *Annu Rev Plant Biol* 60:239–260
- Lichtenthaler HK, Babani F (2004) Light adaptation and senescence of the photosynthetic apparatus. Changes in pigment composition, chlorophyll fluorescence parameters and photosynthetic activity. In: Papageorgiou GC, Govindjee (eds) *Chlorophyll a fluorescence: a signature of photosynthesis*, *Advances in photosynthesis and respiration*, vol 19. Springer, Dordrecht, pp 713–736
- Lin I-J, Chen Y, Fee JA, Song J et al (2006) Rieske protein from *Thermus thermophilus*: ¹⁵N NMR titration study demonstrates the role of iron-ligated histidines in the pH dependence of the reduction potential. *J Am Chem Soc* 128:10672–10673
- Link TA (1997) The role of the “Rieske” iron sulfur protein in the hydroquinone oxidation (Q_p) site of the cytochrome *bc₁* complex: the “proton-gated affinity change” mechanism. *FEBS Lett* 412:257–264
- Malnoë A, Wollman F-A, de Vitry C et al (2011) Photosynthetic growth despite a broken Q-cycle. *Nature Communications* 2:301. <https://doi.org/10.1038/ncomms1299/www.nature.com/naturecommunications>

- Mamedov M, Govindjee, Nadtochenko V et al (2015) Primary electron transfer processes in photosynthetic reaction centers from oxygenic organisms. *Photosynth Res* 125:51–63
- Michelet L, Zaffagnini M, Morisse S et al (2013) Redox regulation of the Calvin–Benson cycle: something old, something new. *Front Plant Sci* 4:Article 470. <https://doi.org/10.3389/fpls.2013.00470>
- Mitchell P (1966) Chemiosmotic coupling in oxidative and photosynthetic phosphorylation. *Biol Rev* 41:445–502
- Mitchell P (1976) Possible molecular mechanisms of the protonmotive function of cytochrome systems. *J Theor Biol* 62:327–367
- Motohashi K, Hisabori T (2006) HCF164 receives reducing equivalents from stromal thioredoxin across the thylakoid membrane and mediates reduction of target proteins in the thylakoid lumen. *J Biol Chem* 281:35039–35047
- Müh F, Glöckner C, Hellmich J et al (2012) Light-induced quinone reduction in photosystem II. *Biochim Biophys Acta* 1817:44–65
- Mulkidjanian AY (2005) Ubiquinol oxidation in the cytochrome *bc₁* complex: reaction mechanism and prevention of short-circuiting. *Biochim Biophys Acta* 1709:5–34
- Munekage Y, Hojo M, Meurer J et al (2002) *PGR5* is involved in cyclic electron flow around photosystem I and is essential for photoprotection in *Arabidopsis*. *Cell* 110:361–371
- Munekage Y, Hashimoto M, Miyake C et al (2004) Cyclic electron flow around photosystem I is essential for photosynthesis. *Nature* 429:579–582
- Munekage Y, Genty B, Peltier G (2008) Effect of *PGR5* impairment on photosynthesis and growth in *Arabidopsis thaliana*. *Plant Cell Physiol* 49:1688–1698
- Nelson N, Yocum CF (2006) Structure and function of photosystems I and II. *Annu Rev Plant Biol* 57:521–565
- Osyczka A, Moser CC, Daldal F et al (2004) Reversible redox energy coupling in electron transfer chains. *Science* 427:607–612
- Osyczka A, Moser CC, Dutton L (2005) Fixing the Q cycle. *Trends Biochem Sci* 30:176–182
- Peng CC, Moser CC, Chen X et al (1999) Natural engineering principles of electron tunnelling in biological oxidation-reduction. *Nature* 402:47–52
- Peng LW, Shimizu H, Shikanai T (2008) The chloroplast NAD(P)H dehydrogenase complex interacts with Photosystem I in *Arabidopsis*. *J Biol Chem* 283:34873–34879
- Peng LW, Fukao Y, Fujiwara M et al (2009) Efficient operation of NAD(P)H dehydrogenase requires supercomplex formation with Photosystem I via minor LHCI in *Arabidopsis*. *Plant Cell* 21:3623–3640
- Pesaresi P, Hertle A, Pribil M et al (2010) Optimizing photosynthesis under fluctuating light. The role of the *Arabidopsis* STN7 kinase. *Plant Signal Behav* 5:21–25
- Pierre Y, Breyton C, Kramer D, Popot J-L (1995) Purification and characterization of the cytochrome *b₆f* complex from *Chlamydomonas reinhardtii*. *J Biol Chem* 270:29342–29349
- Ponamarev MV, Cramer WA (1998) Perturbation of the internal water chain in cytochrome *f* of oxygenic photosynthesis: loss of concerted reduction of cytochromes *f* and *b*. *Biochemistry* 37:17199–17208
- Postila PA, Kaszuba K, Sarewicz M et al (2013) Key role of water in proton transfer at the Q_{0} -site of the cytochrome *bc₁* complex predicted by atomistic molecular dynamics simulations. *Biochim Biophys Acta* 1827:761–768
- Puthiyaveetil S, Kirchhoff H, Hohner R (2016) Structural and functional dynamics of the thylakoid membrane system. In: Kirchhoff H (ed) *Chloroplasts. Current research and future trends*. Caister Academic Press, Norfolk, pp 59–87
- Rich PR (2004) The quinone chemistry of *bc* complexes. *Biochim Biophys Acta* 1658:165–171
- Roberts AG, Bowman MK, Kramer DM (2002) Certain metal ions are inhibitors of cytochrome *b₆f* complex ‘Rieske’ iron-sulfur protein domain movements. *Biochemistry* 41:4070–4079
- Rochaix J-D (2014) Regulation and dynamics of the light-harvesting system. *Annu Rev Plant Biol* 65:287–309

- Ruban A (2012) The photosynthetic membrane: molecular mechanisms and biophysics of light harvesting. Wiley-Blackwell, Oxford
- Rumberg B, Siggel U (1969) pH changes in the inner phase of the thylakoids during photosynthesis. *Naturwissenschaften* 56:130–132
- Sainz G, Carrell CJ, Pomarev MV et al (2000) Interruption of the internal water chain of cytochrome *f* impairs photosynthetic function. *Biochemistry* 39:9164–9173
- Samoilova RI, Kolling D, Uzawa T et al (2002) The interaction of the Rieske iron sulfur protein with occupants of the Q_o-site of the bc₁ complex, probed by 1D and 2D electron spin echo envelope modulation. *J Biol Chem* 277:4605–4608
- Schöttler MA, Tóth SZ, Boulouis A, Kahlau S (2015) Photosynthetic complex stoichiometry dynamics in higher plants: biogenesis, function, and turnover of ATP synthase and the cytochrome *b₆f* complex. *J Exp Bot* 66:2373–2400
- Seelert H, Poetsch A, Dencher NA et al (2000) Structural biology. Proton-powered turbine of a plant motor. *Nature* 405:418–419
- Shelaev IV, Gostev FE, Mamedov MD et al (2010) Femtosecond primary charge separation in photosystem I. *Biochim Biophys Acta* 1797:1410–1420
- Shikanai T (2007) Cyclic electron transport around photosystem I: Genetic approaches. *Plant Biol* 58:199–217
- Shikanai T (2016) Chloroplast NDH: a different enzyme with a structure similar to that of respiratory NADH dehydrogenase. *Biochim Biophys Acta* 1857:1015–1022
- Shikanai T, Endo T, Hashimoto et al (1998) Directed disruption of the tobacco *ndhB* gene impairs cyclic electron flow around photosystem I. *Proc Natl Acad Sci U S A* 95:9705–9709
- Siggel U, Renger G, Stiehl HH et al (1972) Evidence for electronic and ionic interaction between electron transport chains in chloroplasts. *Biochim Biophys Acta*:328–335
- Snyder CH, Gutierrez-Cirlos EB, Trumpower BL (2000) Evidence for a concerted mechanism of ubiquinol oxidation by the cytochrome bc₁ complex. *J Biol Chem* 275:13535–13541
- Soriano GM, Pomarev MV, Tae G-S et al (1996) Effect of the interdomain basic region of cytochrome *f* on its redox reactions *in vivo*. *Biochemistry* 35:14590–14598
- Soriano GM, Guo L-W, de Vitry C et al (2002) Electron transfer from the Rieske iron-sulfur protein (ISP) to cytochrome *f* *in vitro*. Is a guided trajectory of the ISP necessary for competent docking? *J Biol Chem* 277:41865–41871
- Staehelin LA (2003) Chloroplast structure: from chlorophyll granules to supra-molecular architecture of thylakoid membranes. *Photosynth Res* 76:185–196
- Stiehl HH, Witt HT (1969) Quantitative treatment of the function of plastoquinone in photosynthesis. *Z Naturforsch* 24b:1588–1598
- Stirbet A (2013) Excitonic connectivity between photosystem II units: what is it, and how to measure it. *Photosynth Res* 116:189–214
- Strand DD, Fisher N, Kramer DM (2016) Distinct energetics and regulatory functions of the two major cyclic electron flow pathways in chloroplasts. In: Kirchhoff H (ed) *Chloroplasts. Current research and future trends*. Caister Academic Press, Norfolk, pp 89–100
- Stroebel D, Choquet Y, Popot J-L et al (2003) An atypical heme in the cytochrome *b₆f* complex. *Nature* 426:413–418
- Suorsa M, Järvi S, Grieco M et al (2012) PROTON GRADIENT REGULATIONS5 is essential for proper acclimation of *Arabidopsis* photosystem I to naturally and artificially fluctuating light conditions. *Plant Cell* 24:2934–2948
- Tikhonov AN (2013) pH-dependent regulation of electron transport and ATP synthesis in chloroplasts. *Photosynth Res* 116:511–534
- Tikhonov AN (2014) The cytochrome *b₆f* complex at the crossroad of photosynthetic electron transport pathways. *Plant Physiol Biochem* 81:163–183
- Tikhonov AN (2015) Induction events and short-term regulation of electron transport in chloroplasts: an overview. *Photosynth Res* 125:65–94

- Tikhonov AN (2016) Modeling electron and proton transport in chloroplasts. In: Kirchhoff H (ed) Chloroplasts. Current Research and Future Trends. Caister Academic Press, Norfolk, pp 101–134
- Tikhonov AN, Ruuge EK (1979) Electron paramagnetic resonance study of electron transport in photosynthetic systems. VIII. The interplay between two photosystems and kinetics of P700 redox transients under various conditions of flash excitation. *Molec Biol (Moscow)* 13:1085–1097
- Tikhonov AN, Vershetskii AV (2017) Connectivity between electron transport complexes and modulation of photosystem II activity in chloroplasts. *Photosynth Res* 133:103–114
- Tikhonov AN, Khomutov GB, Ruuge EK (1980) Electron spin resonance study of electron transport in photosynthetic systems. IX. Temperature dependence of the kinetics of P700 redox transients in bean chloroplasts induced by flashes with different duration. *Molec Biol (Moscow)* 14:157–172
- Tikhonov AN, Khomutov GB, Ruuge EK et al (1981) Electron transport control in chloroplasts. Effects of photosynthetic control monitored by the intrathylakoid pH. *Biochim Biophys Acta* 637:321–333
- Tikhonov AN, Timoshin AA, Blumenfeld LA (1983) The kinetics of electron transport translocation of protons and photophosphorylation in chloroplasts and their relationship with the thermo-induced structural changes in the thylakoid membrane. *Molec Biol (Moscow)* 17:1236–1248
- Tikhonov AN, Khomutov GB, Ruuge EK (1984) Electron transport control in chloroplasts. Effects of magnesium ions on the electron flow between two photosystems. *Photobiochem Photobiophys* 8:261–269
- Tikkanen M, Aro E-M (2012) Thylakoid protein phosphorylation in dynamic regulation of photosystem II in higher plants. *Biochim Biophys Acta* 1817:232–238
- Tikkanen M, Grieco M, Nurmi M et al (2012) Regulation of the photosynthetic apparatus under fluctuating growth light. *Philos Trans R Soc Lond B* 367:3486–3493
- Tremmel IG, Kirchhoff H, Weis E et al (2003) Dependence of plastoquinol diffusion on the shape, size, and density of integral thylakoid proteins. *Biochim Biophys Acta* 1603:97–109
- Turina P, Petersen J, Gräber P (2016) Thermodynamics of proton transport coupled ATP synthesis. *Biochim Biophys Acta* 1857:653–664
- Vener AV, van Kan PJ, Rich PR et al (1997) Plastoquinol at the quinol oxidation site of reduced cytochrome *b₆f* mediates signal transduction between light and protein phosphorylation: Thylakoid protein kinase deactivation by a single-turnover flash. *Proc Natl Acad Sci U S A* 94:1585–1590
- Victoria D, Burton R, Crofts AR (2013) Role of the –PEWY–glutamate in catalysis at the Q_o-site of the Cyt *b₆f* complex. *Biochim Biophys Acta* 1827:365–386
- Witt HT (1979) Energy conversion in the functional membrane of photosynthesis. Analysis by light pulse and electric pulse methods. The central role of the electric field. *Biochim Biophys Acta* 505:355–427
- Wood PM (1988) The potential diagram for oxygen at pH 7. *Biochem J* 253:287–289
- Xia D, C-A Y, Kim H et al (1997) Crystal structure of the cytochrome *b₆f* complex from bovine heart mitochondria. *Science* 277:60–66
- Xia D, Esser L, Tang W-K et al (2013) Structural analysis of cytochrome *b₆f* complexes: Implications to the mechanism of function. *Biochim Biophys Acta* 1827:1278–1294
- Yamashita E, Zhang H, Cramer WA (2007) Structure of the cytochrome *b₆f* complex: Quinone analogue inhibitors as ligands of heme *c_n*. *J Mol Biol* 370:39–52
- Yamori W, Shikanai T (2016) Physiological functions of cyclic electron transport around photosystem I in sustaining photosynthesis and plant growth. *Annu Rev Plant Biol* 67:81–106
- Yan J, Cramer WA (2003) Functional insensitivity of the cytochrome *b₆f* complex to structure changes in the hinge region of the Rieske iron–sulfur protein. *J Biol Chem* 278:20926–20933
- Zhang H, Carrell CJ, Huang D et al (1996) Characterization and crystallization of the lumen side domain of the chloroplast Rieske iron–sulfur protein. *J Biol Chem* 271:31360–31366

- Zhang Z, Huang L, Shulmeister VM et al (1998) Electron transfer by domain movement in cytochrome *bc*₁. *Nature* 392:677–684
- Zhang H, Whitelegge JP, Cramer WA (2001) Ferredoxin: NADP⁺ oxidoreductase is a subunit of the chloroplast cytochrome *b₆f* complex. *J Biol Chem* 276:38159–38165
- Zhu J, Egawa T, Yeh S-R et al (2007) Simultaneous reduction of iron-sulfur protein and cytochrome *b_L* during ubiquinol oxidation in cytochrome *bc*₁ complex. *Proc Natl Acad Sci U S A* 104:4864–4869
- Zito F, Finazzi G, Joliot P et al (1998) Glu78, from the conserved PEWY sequence of subunit IV, has a key function in the cytochrome *b₆f* turnover. *Biochemistry* 37:10395–10403
- Zito F, Finazzi G, Delosme R et al (1999) The Q_o site of cytochrome *b₆f* complexes controls the activation of the LHCII kinase. *EMBO J* 18:2961–2969
- Zu Y, Manon M-J, Couture MM-J et al (2003) Reduction potentials of Rieske clusters: Importance of the coupling between oxidation state and histidine protonation state. *Biochemistry* 42:12400–12408